Journal of Statistical Physics, Vol. 67, Nos. 1/2, 1992

The Asymmetric Six-Vertex Model

I. M. Nolden[1, 2]

Received July 29, 1991

The exact solution of the asymmetric six-vertex model, published nearly without derivation by Sutherland *et al.* in 1967, is rederived in detail. The transfer matrix method and the Bethe Ansatz solution for the free energy (which can be calculated from an integral equation) are discussed. For some special cases (zero or maximal polarization) the integral equation can be solved exactly. In addition, an asymptotic analysis, valid for small but nonzero polarization, is carried out. The analytical properties of the results and their relevance for the BCSOS model are discussed.

KEY WORDS: Six-vertex model; transfer matrix; Bethe Ansatz; BCSOS model.

The six-vertex model was introduced by Slater[1] to describe the thermodynamical behavior of certain 3-dimensional crystals, such as ice and potassium dihydrogen phosphate (KDP). The essential property these crystals have in common is that the oxygen groups in ice and the phosphate groups in KDP form a lattice of coordination number four, with a hydrogen atom between each pair of lattice sites. Assuming local electric neutrality, Slater proposed the so-called *ice rule*: each lattice site should have two hydrogen atoms near to it and two a bit further removed from it. One easily verifies that the four hydrogen atoms surrounding a given lattice site can be arranged in precisely *six* different ways. Slater further proposed that the thermodynamic properties of crystals like ice and KDP could be studied from a 2-dimensional model, where the six possible arrangements of the hydrogen atoms are represented by six different vertices. The resulting so-called six-vertex model was first solved by Lieb[2] for

[1] Institute for Theoretical Physics, Princetonplein 5, 3508 TA Utrecht, The Netherlands.
[2] Present address: Department of Chemistry, Massachusetts Institute of Technology, Cambridge, Massachusetts 02139.

0022-4715/92/0400-0155$06.50/0

important special values of the vertex energies. The general, or asymmetric, six-vertex model was then solved by Sutherland.[3] Further results were published in ref. 4.

However, apart from the results that were published almost without derivation by Sutherland *et al.*,[4] there exists in the literature only a partial treatment of the asymmetric six-vertex model by Lieb and Wu[5] and of course an exact solution of the symmetric six-vertex model by Lieb.[2] The fact that a detailed solution is lacking in the literature is extremely unfortunate, since this hampers the study of related models. In particular, the direct motivation for this work is that several microscopic models for the equilibrium shape of crystals[6–8] can be mapped exactly onto the six-vertex model. A prerequisite for the study of these models for equilibrium crystal shapes is therefore that the solution of the six-vertex model is well understood. For this reason we discuss the asymmetric six-vertex model in detail below. The methods and results presented in this paper will form the basis for the analytical and numerical studies of equilibrium crystal shapes which will be published elsewhere.[9, 10]

This paper is organized as follows. In Section 1 we give a brief introduction to the six-vertex model, where the notations and definitions used in this paper are explained and some general properties are discussed. The method of solution, i.e., the calculation of the free energy with the help of the transfer matrix method and the Bethe Ansatz, is presented in Section 2. The equation for the free energy is analyzed in Sections 3–5. The antiferroelectric phase of the model is discussed in Section 3, the paraelectric phase in Section 4. Section 5 contains results concerning the phase with maximal polarization. A summary is given in Section 6. Technical details are treated in Appendices A–E.

1. INTRODUCTION TO THE SIX-VERTEX MODEL

Consider a two-dimensional quadratic lattice with N sites in the horizontal and M sites in the vertical direction. The hydrogen bonds between the atoms on the lattice sites (the vertices) form electric dipoles and hence can be represented by arrows on the lattice bonds, e.g., $--H-$ can be represented by $\rightarrow$. For each vertex there are 16 possible configurations of the four bonds, but only the 6 configurations with two arrows pointing in and two arrows pointing out satisfy the ice rule (see Fig. 1). In Fig. 2 we give examples for configurations of the six-vertex model with periodicity in the horizontal direction. Yang[4] showed that the most general, the so-called asymmetrix six-vertex model, where all vertices have different energies, is equivalent to the symmetric six-vertex model in the presence of an external electric field. (The field removes the symmetry with respect to

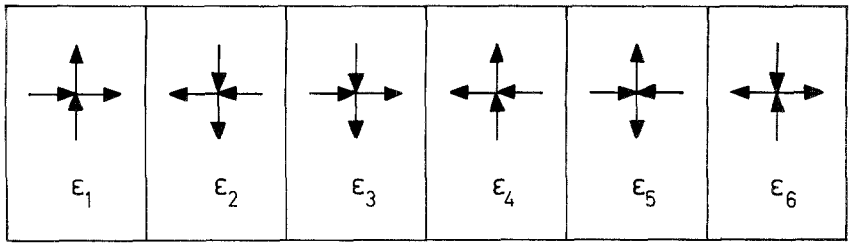

Fig. 1. The allowed six-vertex configurations.

reversing all dipoles.) If the energies of horizontal and vertical dipoles in the horizontal and vertical electric fields are denoted by $2h$ and $2v$, respectively, the following energies for the six allowed vertices are obtained (see also Fig. 1):

$$\begin{aligned}
\varepsilon_1 &= -\tfrac{1}{2}\delta \quad -h \quad -v \\
\varepsilon_2 &= -\tfrac{1}{2}\delta \quad +h \quad +v \\
\varepsilon_3 &= \tfrac{1}{2}\delta \quad -h \quad +v \\
\varepsilon_4 &= \tfrac{1}{2}\delta \quad +h \quad -v \\
\varepsilon_5 &= -\varepsilon \\
\varepsilon_6 &= -\varepsilon
\end{aligned} \tag{1.1}$$

Note that $\varepsilon_5 = \varepsilon_6$ does not mean any restriction. It is obvious that vertex 5 is a sink of horizontal arrows and vertex 6 a source. Because of the horizontal periodicity, the numbers of sources and sinks must be equal (see Fig. 2) and hence their energies occur in the total energy of a six-vertex configuration only in the combination $\varepsilon_5 + \varepsilon_6$.[11] It can also easily be seen

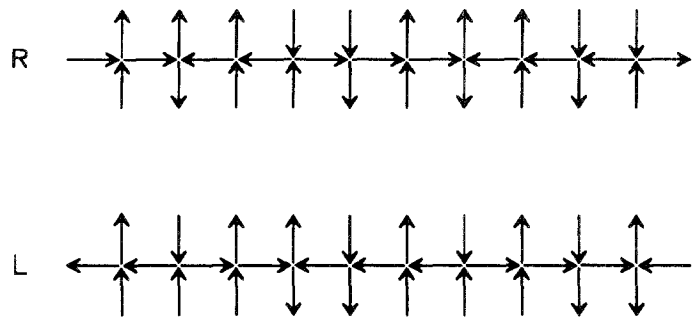

Fig. 2. Example for corresponding R- and L-configurations.

that the number of down arrows n (or up arrows $N-n$) must be equal in each row of vertical bonds in order to obtain vertex configurations which satisfy both the ice rule and the horizontal periodicity. It will turn out that the conservation of n is essential for the solubility of the asymmetric six-vertex model. An additional consequence of the ice rule is that vertices 5 and 6 must occur alternately.

Before dealing with the method that can be used to calculate the partition function of this model, we discuss the physical properties that can already be obtained from the vertex energies (1.1). First we define a few useful quantities:

$$\eta \equiv \exp(\beta\delta) \tag{1.2}$$

$$\Delta \equiv \tfrac{1}{2}[\eta + \eta^{-1} - \exp(2\beta\varepsilon)] \tag{1.3}$$

$$H \equiv \exp(2\beta h) \tag{1.4}$$

$$V \equiv \exp(2\beta v) \tag{1.5}$$

with $\beta = 1/kT$, where k is Boltzmann's constant and T the temperature.

Consider the vertex energies (1.1) for vanishing electric fields ($h = v = 0$). There are two types of models possible, depending on whether the vertices 5 and 6 with zero net polarization have the lowest energy or the vertices with nonvanishing net polarization (vertices 1 and 2 or vertices 3 and 4). The first type has two degenerate antiferroelectric ground states in zero field (with alternating vertices 5 and 6). The second type has two degenerate ferroelectric ground states with opposite polarizations according to the net polarizations of the vertices 1 or 2 (or 3 or 4, respectively). If we concentrate, for example, upon nonnegative values for δ, the first type, called intrinsically antiferroelectric,[5] occurs for $\varepsilon > \frac{1}{2}\delta \geqslant 0$ and the second, intrinsically ferroelectric, for $\varepsilon \leqslant \frac{1}{2}\delta$. (Vertices 3 and 4 can only obtain the lowest energy in zero field if δ is chosen negative. This case is discussed in ref. 5.). These two model types correspond to complementary ranges for Δ as a function of the temperature. One observes the following behavior:

1. For intrinsically antiferroelectric models

$$\Delta \uparrow \tfrac{1}{2} \qquad \text{if} \quad T \to \infty$$

$$\Delta \to -\infty \qquad \text{if} \quad T \to 0$$

2. For intrinsically ferroelectric models

$$\Delta \downarrow \tfrac{1}{2} \qquad \text{if} \quad T \to \infty$$

$$\Delta \to \infty \qquad \text{if} \quad T \to 0$$

From the vertex energies in the presence of an electric field (1.1) one can obtain the ($T=0$) phase diagram of the six-vertex model in the (h, v) plane. By comparing the energies $\varepsilon_1, \varepsilon_2, ..., \varepsilon_6$ one can find out in which region of the (h, v) plane a given vertex has the lowest energy.[5] Figure 3 shows an example of such a phase diagram with $\varepsilon > \frac{1}{2}\delta > 0$. Region 5, where vertices 5 and 6 occur alternately, is a rectangle the short sides of which have a length proportional to $\sqrt{2}\,(\varepsilon - \frac{1}{2}\delta)$ and the long sides of which have a length proportional to $\sqrt{2}\,(\varepsilon + \frac{1}{2}\delta)$. Note that the isotropic model (the so-called F-model) occurs for $\delta = 0$, while the extremely anisotropic model occurs in the limit $(\varepsilon - \frac{1}{2}\delta) \to 0$. The corresponding phase diagram for the ferroelectric model can be obtained in the same way.[5] In spite of these different physical properties depending on the values of δ and ε, the asymmetric six-vertex model can be solved for both model types simultaneously, as we shall see in the next section.

The vertex energies (1.1) show also that the six-vertex model in the presence of an electric field is symmetric with respect to reversing all arrows *and* the electric field. Hence we conclude that its free energy $F(h, v)$ has the following symmetry:

$$F(h, v) = F(v, h) = F(-h, -v) = F(-v, -h) \tag{1.6}$$

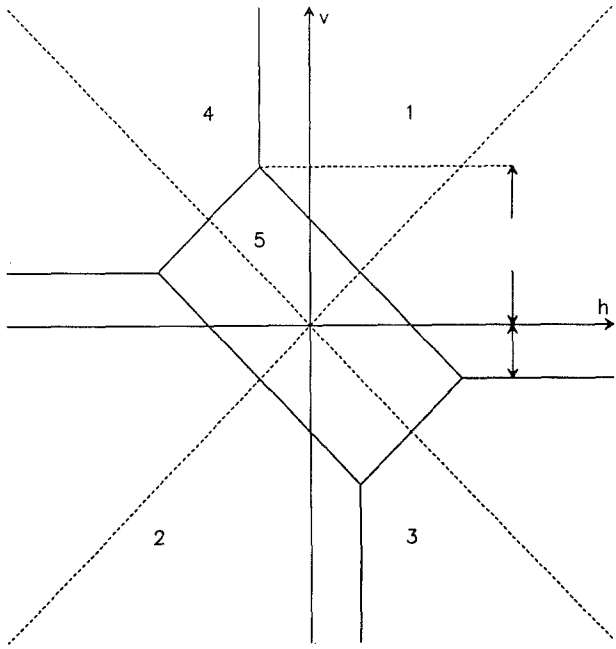

Fig. 3. ($T=0$) phase diagram for an intrinsically antiferroelectric model with $\varepsilon > \frac{1}{2}\delta > 0$.

Thus, the free energy can be obtained in the entire (h, v) plane from the free energy in the region $v \geqslant |h|$. The physics of the model can be described alternatively with the help of the Legendre transform of $F(h, v)$, the free energy $F(x, y)$ as a function of the horizontal and vertical polarizations x and y per horizontal and vertical bond, respectively. The vertical polarization per vertical bond can be defined in terms of N and n as follows:

$$y = \frac{N - 2n}{N} \tag{1.7}$$

In the thermodynamic limit $(N \to \infty)$, y will become a continuous quantity. It follows directly from the definition that $-1 \leqslant y \leqslant 1$. The horizontal polarization can be interpreted in an analogous way, with $-1 \leqslant x \leqslant 1$, however, not formulated in a simple way like y. In terms of x and y, $F(x, y)$ shows the same symmetry as $F(h, v)$.[4] The method of solution of the six-vertex model, however, will lead to the free energy depending on h and y, as will be shown in the next section. The functions $F(x, y)$ and $F(h, v)$ can be obtained from this result by the following Legendre transformations:

$$F(x, y) = F(h, y) + hx \tag{1.8}$$

with

$$x = -\left.\frac{\partial F(h, y)}{\partial h}\right|_y \tag{1.9}$$

and

$$F(h, v) = F(h, y) - vy \tag{1.10}$$

with

$$v = \left.\frac{\partial F(h, y)}{\partial y}\right|_h \tag{1.11}$$

Note that all three free energies are defined per lattice site.

2. METHOD OF SOLUTION

2.1. The Transfer Matrix Method

In this section we sketch the so-called transfer matrix method which can be used to calculate the partition function of the asymmetric six-vertex

model. A detailed treatment is given by Lieb,[2] Lieb and Wu,[5] or Baxter,[11] for example.

One chooses periodic boundary conditions in the horizontal and vertical directions. Consider now a row of N vertical bonds. A state of such a row (with index k) is the configuration of up or down arrows on these bonds, denoted by ϕ_k. Next one defines the transfer matrix $\mathbf{T}$ with elements $T_{kl}=\sum' \exp(-\beta E_{kl})$ which couple the states of two adjacent rows with configurations ϕ_k and ϕ_l. The sum $\sum'$ is over all configurations of the horizontal bonds that are allowed by the ice rule and the periodic boundary conditions. The energy E_{kl} is the sum of the vertex energies for the vertices so obtained. It is easy to show that the partition function Z can be written in terms of the transfer matrix as follows:

$$Z=\mathrm{Trace}(\mathbf{T}^M)=\sum_{j=1}^{2^N}(\Lambda_j)^M \tag{2.1}$$

where the Λ_j are the eigenvalues of $\mathbf{T}$. In the thermodynamic limit $(M, N\to\infty)$ one obtains from Eq. (2.1)

$$\lim_{N,M\to\infty}\frac{1}{MN}\ln Z=\lim_{N\to\infty}\left(\frac{1}{N}\max_j(\ln\Lambda_j)\right)\equiv\lim_{N\to\infty}\frac{1}{N}\ln\Lambda \tag{2.2}$$

The problem of calculating the partition function has thus been reduced to determining the maximal eigenvalue of the transfer matrix.

As explained in the previous section, the number of down arrows n must be the same in two adjacent rows of vertical bonds. For that reason $T_{kl}=0$ unless ϕ_k and ϕ_l have the same number of down arrows. Thus, $\mathbf{T}$ is a block diagonal matrix with blocks of dimension $\binom{N}{n}$ for given n $(0\leqslant n\leqslant N)$ and the eigenvalue equation for $\mathbf{T}$ can be solved in each block separately. Each configuration with given n can be characterized by the positions of the down arrows,

$$1\leqslant x_1<x_2<\cdots<x_n\leqslant N \tag{2.3}$$

Furthermore, for each R-combination of two rows of vertical bonds with $x_{i-1}\leqslant y_i\leqslant x_i$ (leading to a row of vertices whose first and last horizontal arrows are oriented to the right) one can construct an L-combination (leading to a row of vertices whose first and last horizontal bonds point to the left) with $x_i\leqslant y_i\leqslant x_{i+1}$ by exchanging the two rows of vertical bonds and reversing all horizontal bonds (see Fig. 2 for an example). Therefore, the transfer matrix can be written as a sum of two terms,

$$\mathbf{T}=\mathbf{T}^{\mathrm{R}}+\mathbf{T}^{\mathrm{L}}$$

Explicit expressions for the elements of the transfer matrix $T_{kl}^{R,L}$ are given by Lieb and Wu.[5] In general, **T** is a real but not a symmetric matrix. In a given subspace n one obtains for the logarithm of the partition function

$$\lim_{M,N\to\infty} \frac{1}{MN} \ln Z(n) = \lim_{N\to\infty} \left[\frac{1}{N} \max_{R,L} (\ln \Lambda_R(n), \ln \Lambda_L(n)) \right] \tag{2.4}$$

In the thermodynamic limit $M, N \to \infty$, while $n/N = \text{const}$, it is convenient to replace the discrete n by the continuous vertical polarization per vertical bond y [defined by Eq. (1.7)]. Thus, one obtains from Eq. (2.4) the free energy per lattice site of the six-vertex model as a function of y (and h, the dipole energy in the horizontal electric field).

To find the maximal eigenvalue of **T** in a subspace n, i.e., the free energy, two methods have been used. The older one has been developed by Lieb[2] for two-dimensional ice (a six-vertex model with all vertex energies equal to zero). This method works as follows. According to the Perron–Frobenius theorem,[12] the only eigenvector of the transfer matrix in subspace n with real nonnegative coefficients is the one corresponding to the (nondegenerate) maximal eigenvalue. For this eigenvector one makes the following Bethe Ansatz:

$$\psi(x_1, \ldots, x_N) = \sum_P A(P) \exp\left(i \sum_{j=1}^{n} k_{P_j} x_j \right) \tag{2.5}$$

where the sum is over the $n!$ permutations P. The n wave numbers k are chosen to be distinct modulo 2π, the amplitudes A are complex functions defined on the permutations P, and the x_i obey (2.3). Substitution of this Ansatz into the eigenvalue equation of **T** in subspace n yields one term proportional to the Ansatz that can be identified with the desired maximal eigenvalue, provided that the remaining terms are equal to zero. This condition leads to n consistency equations for the n wave numbers k and, in addition, to certain conditions on the amplitudes A. This is a lengthy procedure. The second method is much more elegant. Jayaprakash and Sinha[13] use Baxter's commuting transfer matrix technique to *construct* the eigenvectors of the transfer matrix. (Note that the asymmetric six-vertex model is not contained as a special case in Baxter's solution of the eight-vertex model.) The maximal eigenvalue $\Lambda(n)$ as well as the system of consistency equations then follow immediately.

2.2. Calculation of the Free Energy

From both methods one obtains for the maximal eigenvalue in the subspace n

$$\Lambda(n) \equiv \Lambda_{\mathrm{R}}(n) + \Lambda_{\mathrm{L}}(n) = (H\eta)^{N/2} \prod_{j=1}^{n} \frac{2\Delta - \eta - H\exp(ik_j)}{1 - \eta H \exp(ik_j)}$$
$$+ (H\eta)^{-N/2} \prod_{j=1}^{n} \frac{2\Delta - \eta^{-1} - H^{-1}\exp(-ik_j)}{1 - \eta^{-1}H^{-1}\exp(-ik_j)} \tag{2.6}$$

where the wavenumbers k_j $(1 \leqslant j \leqslant n)$ of the Bethe Ansatz (2.5) obey the following system of consistency equations:

$$\exp(ik_l N) = (-1)^{n-1} \prod_{\substack{j=1 \\ j \neq l}}^{n} \frac{1 + H^2 \exp[i(k_j + k_l)] - 2\Delta H \exp(ik_l)}{1 + H^2 \exp[i(k_j + k_l)] - 2\Delta H \exp(ik_j)} \tag{2.7}$$

[The definition of Δ is given in Eq. (1.3).]

Now one has to solve the consistency equations (2.7) and to substitute the solution into Eq. (2.6) to calculate the maximal eigenvalue $\Lambda(n)$ explicitly. Following the method of Sutherland *et al.*,[4] one defines a complex variable $p_j^0 = k_j - i \ln H$. In terms of this new variable (2.7) has the same form as the corresponding system of equations for the one-dimensional quantum Heisenberg chain,[14] albeit with complex wavenumbers p_j^0. Hence one can adopt the method used there. Following the lines of ref. 14, we introduce the function $\Theta(p_j^0, p_l^0)$ by rewriting the RHS of Eq. (2.7) as

$$\exp(ip_l^0 N) = H^N (-1)^{n-1} \prod_{j=1}^{n} \exp[i\Theta(p_l^0, p_j^0)] \tag{2.8}$$

The explicit form of this function is given in ref. 14. Because of $\Theta(p_l^0, p_l^0) = 0$ the restriction $j \neq l$ can be lifted. For the logarithm of (2.7) in the rewritten form one then obtains

$$p_l^0 = -i \ln H + \frac{1}{N} I_l + \frac{1}{N} \sum_{j=1}^{n} \Theta(p_l^0, p_j^0), \qquad 1 \leqslant l \leqslant n \tag{2.9}$$

where the term $I_l = \pi(2l - n - 1)$ arises from the choice of a phase factor $(-1)^{n-1} = \exp[i\pi(2l - n - 1)]$. Note that the I_l are arranged symmetrically with respect to the origin between $(-n+1)$ and $(n-1)$.

An explicit solution of Eq. (2.9) is only possible in the thermodynamic limit, $M, N \to \infty$ with $n/N = \text{const}$. One then assumes[4] that the n numbers $\{p^0\}$ lie densely on a smooth curve C in the complex plane, which is symmetric with respect to the imaginary axis and has endpoints Q and $-Q^*$. Hence, the number of p^0's in any interval dp^0 along C is $N\rho(p^0)\,dp^0$ written in terms of a distribution function $\rho(p^0)$. Next one defines a function $f(p^0)$

such that $df/dp^0 = \rho(p^0)$ along C with $f = 0$ at the midpoint of C. The normalization of the distribution function can be expressed in terms of f:

$$\int_C \rho(p^0)\, dp^0 = \frac{n}{N} = \frac{1}{2}(1 - y) = f(Q) - f(-Q^*) \tag{2.10}$$

[From now on we shall use the vertical polarization per vertical bond y, which was defined by Eq. (1.7), instead of the discrete variable n.] In the new continuous variables p^0 and q^0, Eq. (2.9) can be written as

$$2\pi f(p^0) - i \ln H = p^0 - \int_C \Theta(p^0, q^0)\, \rho(q^0)\, dq^0 \tag{2.11}$$

Note that the function f takes the role of I_l in (2.9). By differentiation with respect to p^0 one obtains from (2.11) the following integral equation for the distribution function $\rho(p^0)$:

$$2\pi\rho(p^0) + \int_C \frac{\partial\Theta(p^0, q^0)}{\partial p^0}\, \rho(q^0)\, dq^0 = 1 \tag{2.12}$$

The solution of this integral equation is the first crucial step to calculate the free energy from the fundamental equation (2.4) with Λ_R and Λ_L from (2.6):

$$\begin{aligned} -\beta F(h, y) &= \lim_{M,N\to\infty} \frac{1}{MN} \ln Z(h, n) \\ &= \lim_{N\to\infty} \left[\frac{1}{N} \max_{R,L} (\ln \Lambda_R(h, y), \ln \Lambda_L(h, y)) \right] \end{aligned} \tag{2.13}$$

where we replace the summation by an integral over $\rho(p^0)\, dp^0$ in the thermodynamic limit. To achieve this goal one uses a further transformation from complex variables (p^0, q^0) to complex variables (α, β) (see Table I). By that means the kernel of (2.12) is transformed to a difference kernel $K(\alpha - \beta)$, the structure of which in some cases allows for exact solution in closed form. A consequence of this method is that one has to use different transformations in the intervals $\Delta < -1$, $-1 < \Delta < 1$, and $1 < \Delta$ and for $\Delta = -1$ and $\Delta = 1$. These transformations have been given.[4, 14] As we shall see later, this splitting of the Δ range (i.e., the temperature range) has a deeper physical reason, namely a qualitative change in the behavior of the model.

In this paper we restrict ourselves to $\Delta < 1$ because we are mainly interested in the applications of intrinsically antiferroelectric models where $-\infty < \Delta < \frac{1}{2}$ (see above). Note, however, that the solution derived here for

$-1 < \Delta < 1$ contains also the high-temperature behavior of the intrinsically ferroelectric models (where $\frac{1}{2} < \Delta < 1$).

Under the transformation from (p^0, q^0) to (α, β) the integration path C is mapped onto a curve C' with endpoints $(-a+ib)$ and $(a+ib)$. The maximum range of the parameter a depends on Δ: $0 \leqslant a \leqslant \pi$ if $\Delta < -1$ and $0 \leqslant a < \infty$ if $-1 \leqslant \Delta < 1$ (see Table I). Next we define a distribution function for the new variable α along the curve C' by $R(\alpha)\, d\alpha = 2\pi\rho(p^0)\, dp^0$. In terms of the new variables the integral equation (2.12) then takes the following form:

$$R(\alpha) + \frac{1}{2\pi} \int_{-a+ib}^{a+ib} K(\alpha - \beta)\, R(\beta)\, d\beta = \xi(\alpha) \tag{2.14}$$

where the kernel is defined by

$$K(\alpha - \beta) \equiv \frac{d\Theta(\alpha - \beta)}{d(\alpha - \beta)} \tag{2.15}$$

and the inhomogeneity by

$$\xi(\alpha) \equiv \frac{dp^0(\alpha)}{d\alpha} \tag{2.16}$$

The normalization of the distribution function $R(\alpha)$ follows from Eq. (2.10),

$$\int_{-a+ib}^{a+ib} R(\alpha)\, d\alpha = \pi(1 - y) \tag{2.17}$$

Since $R(\alpha)$ is an analytic function of α, one can replace the integration path C' by one parallel to the real axis with endpoints $(-a+ib)$ and $(a+ib)$. In this case we can conclude from Eq. (2.17) that the real part of $R(\alpha)$ is a symmetric function of $Re(\alpha)$, while the imaginary part of $R(\alpha)$ is antisymmetric in this variable:

$$R(-\alpha^*) = R^*(\alpha)$$

Furthermore, we can conclude from (2.17) that y must be a monotonically decreasing function of a. Besides (2.14), we obtain the following equations. Equation (2.11) is transformed to

$$g(\alpha) = p^0(\alpha) - \frac{1}{2\pi} \int_{-a+ib}^{a+ib} \Theta(\alpha - \beta)\, R(\beta)\, d\beta \tag{2.18}$$

Table I. Explicit Expressions for the Transformation from p^0 to α and for the Functions Θ, K, ρ^0, ξ, and $\Phi^{R,L}$ for the Cases $-1<\Delta<1$, $\Delta=-1$, and $\Delta<-1$

	$-1<\Delta<1$	$\Delta=-1$	$\Delta<-1$
$\Delta=$	$-\cos\mu,\ 0<\mu<\pi$	-1	$-\cosh\lambda,\ \lambda>0$
Range of $Re(p^0)$	$(-\pi+\mu,\ \pi-\mu)$	$(-\pi,\ \pi)$	$(-\pi,\ \pi)$
$e^{ip^0}=$	$\dfrac{e^{i\mu}-e^{\alpha}}{e^{i\mu+\alpha}-1}$	$\dfrac{1+2i\alpha}{1-2i\alpha}$	$\dfrac{e^{\lambda}-e^{-i\alpha}}{e^{\lambda-i\alpha}-1}$
Range of a	$(0,\ \infty)$	$(0,\ \infty)$	$(0,\ \pi)$
$\Theta(\alpha,\beta)=$	$2\arctan\left[\cot\mu\cdot\tanh\left(\dfrac{\alpha-\beta}{2}\right)\right]$	$2\arctan(\alpha-\beta)$	$2\arctan\left[\coth\lambda\cdot\tan\left(\dfrac{\alpha-\beta}{2}\right)\right]$
Range of Θ	$(-\lvert\pi-2\mu\rvert,\ \lvert\pi-2\mu\rvert)$	$(-\pi,\ \pi)$	$(-2\pi,\ 2\pi)$
$K(\alpha-\beta)=$	$\dfrac{\sin 2\mu}{\cosh(\alpha-\beta)-\cos 2\mu}$	$\dfrac{2}{1+(\alpha-\beta)^2}$	$\dfrac{\sinh 2\lambda}{\cosh 2\lambda-\cos(\alpha-\beta)}$
$\xi(\alpha)=$	$\dfrac{\sin\mu}{\cosh\alpha-\cos\mu}$	$\dfrac{4}{1+4\alpha^2}$	$\dfrac{\sinh\lambda}{\cosh\lambda-\cos\alpha}$
Definition of ϕ_0	$e^{i\phi_0}=\dfrac{1+\eta e^{i\mu}}{e^{i\mu}+\eta},\ 0\leqslant\phi_0\leqslant\mu$	$\phi_0=\dfrac{1}{2}\dfrac{\eta-1}{\eta+1},\ 0\leqslant\phi_0\leqslant\dfrac{1}{2}$	$e^{\phi_0}=\dfrac{1+e^{\lambda}\eta}{e^{\lambda}+\eta},\ 0\leqslant\phi_0\leqslant\lambda$
$\Phi^{R}(\alpha)=$	$\ln\left(\dfrac{e^{\alpha}-e^{i(-2\mu+\phi_0)}}{e^{i\phi_0}-e^{\alpha}}\right)+i\mu$	$\ln\left(\dfrac{1-\phi_0-i\alpha}{\phi_0+i\alpha}\right)$	$\ln\left(\dfrac{e^{-i\alpha}-e^{-2\lambda+\phi_0}}{e^{\phi_0}-e^{-i\alpha}}\right)+\lambda$
$\Phi^{L}(\alpha)=$	$\ln\left(\dfrac{e^{\alpha}-e^{i(2\mu+\phi_0)}}{e^{i\phi_0}-e^{\alpha}}\right)-i\mu$	$\ln\left(\dfrac{1+\phi_0+i\alpha}{-\phi_0-i\alpha}\right)$	$\ln\left(\dfrac{e^{2\lambda+\phi_0}-e^{-i\alpha}}{e^{-i\alpha}-e^{\phi_0}}\right)-\lambda$

Here the function $g(\alpha)$ is defined as the transformed LHS of Eq. (2.11). The values of y and $\ln H$ as functions of the parameters a and b can be calculated from the value of $g(a+ib)$, which will be referred to as the generalized normalization,

$$g(a+ib) = p^0(a+ib) - \frac{1}{2\pi}\int_{-a+ib}^{a+ib} \Theta(a+ib-\beta)\, R(\beta)\, d\beta$$

$$= \frac{\pi}{2}[1 - y(a, b)] - i \ln H(a, b) \tag{2.19}$$

For the free energy we obtain in terms of the new variables from (2.13)

$$-\beta F(h, y) = \max_{R,L}\left[\pm\frac{1}{2}(\ln \eta + \ln H) + \frac{1}{2\pi}\int_{-a+ib}^{a+ib} \Phi^{R,L}(\alpha)\, R(\alpha)\, d\alpha \right] \tag{2.20}$$

where the $(+)$ sign and Φ^R correspond to $\ln \Lambda_R$, while the $(-)$ sign and Φ^L correspond to $\ln \Lambda_L$. The integrals occurring in Eqs. (2.14) and (2.18)–(2.20) can also be taken over a path parallel to the real axis between $(-a+ib)$ and $(a+ib)$ instead of C'. Complications arising from singularities of $\Phi^{R,L}$ will be treated later. Explicit expressions for the transformation from p^0 to α as well as for the functions Θ, K, p^0, ξ, and $\Phi^{R,L}$ are given in Table I for the three cases $-1 < \Delta < 1$, $\Delta = -1$, and $\Delta < -1$. Note that the free energy depends explicitly on the quantities δ, T, Δ, a, and b.

Finally, we introduce the transformation $u = \alpha - ib$ $(v = \beta - ib)$ to obtain integrals running over the real axis with $-a \leqslant u \leqslant a$. The transformed equations in terms of the variable u will be the starting point for the analytical solution described in Section 3 and for the numerical work.[10] After the transformation from α to u the functions p^0, ξ, g, etc., depend explicitly on the parameter b. To mark the difference we denote the functions of the new variable u, for example, by $p^0(u, b)$ [instead of $p^0(\alpha)$], etc. Further note that $\alpha - \beta = u - v$ is a real number. Using this transformation from α to u, we obtain for the integral equation

$$R(u, b) + \frac{1}{2\pi}\int_{-a}^{a} K(u-v)\, R(v, b)\, dv = \xi(u, b) \tag{2.21}$$

for the generalized normalization

$$g(a, b) = p^0(a, b) - \frac{1}{2\pi}\int_{-a}^{a} \Theta(a-v)\, R(v, b)\, dv$$

$$= \frac{\pi}{2}[1 - y(a, b)] - i \ln H(a, b) \tag{2.22}$$

and for the free energy

$$-\beta F(h, y) = \max_{\mathrm{R,L}} \left[\pm\frac{1}{2}(\ln \eta + \ln H) + \frac{1}{2\pi}\int_{-a}^{a} \Phi^{\mathrm{R,L}}(u, b)\, R(u, b)\, du \right] \quad (2.23)$$

Besides the free energy $F(h, y)$, we are interested in its Legendre transforms $F(x, y)$, (1.8), and $F(h, v)$, (1.10). To obtain these quantities we have to calculate the y and h derivatives of $F(h, y)$. Since $F(h, y)$ depends implicitly on h and y through a and b, the differentiation has to be carried out by applying the chain rule.

$$\begin{aligned} \left.\frac{\partial F}{\partial h}\right|_y &= \left.\frac{\partial F}{\partial a}\right|_b \left.\frac{\partial a}{\partial h}\right|_y + \left.\frac{\partial F}{\partial b}\right|_a \left.\frac{\partial b}{\partial h}\right|_y \\ \left.\frac{\partial F}{\partial y}\right|_h &= \left.\frac{\partial F}{\partial a}\right|_b \left.\frac{\partial a}{\partial y}\right|_h + \left.\frac{\partial F}{\partial b}\right|_a \left.\frac{\partial b}{\partial y}\right|_h \end{aligned} \quad (2.24)$$

For simplicity of notation we shall use abbreviations $\partial_a F$ for $(\partial F/\partial a)|_b$, etc., from now on. The derivatives $\partial_a F$ and $\partial_b F$ can be obtained by differentiating Eq. (2.23) with respect to a and b,

$$\begin{aligned} -\beta\, \partial_a F(h, y) = \pm\frac{1}{2}\partial_a \ln H + \frac{1}{2\pi}[&\Phi^{\mathrm{R,L}}(a, b)\, R(a, b) \\ &+ \Phi^{\mathrm{R,L}}(-a, b)\, R(-a, b)] + \frac{1}{2\pi}\int_{-a}^{a} \Phi^{\mathrm{R,L}}(u, b)\, \partial_a R(u, b)\, du \end{aligned} \quad (2.25)$$

$$\begin{aligned} -\beta\, \partial_b F(h, y) = \pm\frac{1}{2}\partial_b \ln H + \frac{1}{2\pi}\int_{-a}^{a} [&\Phi^{\mathrm{R,L}}(u, b)\, \partial_b R(u, b) \\ &+ \partial_b \Phi^{\mathrm{R,L}}(u, b)\, R(u, b)]\, du \end{aligned} \quad (2.26)$$

The derivatives of a and b with respect to h and y can be expressed through the derivatives of h and y with respect to a and b as follows:

$$\begin{pmatrix} \partial_y a & \partial_h a \\ \partial_y b & \partial_h b \end{pmatrix} = \frac{1}{\partial_a y\, \partial_b h - \partial_b y\, \partial_a h} \begin{pmatrix} \partial_b h & -\partial_b y \\ -\partial_a h & \partial_a y \end{pmatrix} \quad (2.27)$$

The derivatives of h and y with respect to a and b are easily obtained from the derivatives of $g(a, b)$ [Eq. (2.22)] with respect to a and b,

$$\begin{aligned} \partial_a g(a, b) &= -\frac{\pi}{2}\partial_a y - i\, \partial_a \ln H \\ &= R(a, b) - \frac{1}{2\pi}\Theta(2a)\, R(-a, b) - \frac{1}{2\pi}\int_{-a}^{a} \Theta(a - v)\, \partial_a R(v, b)\, dv \end{aligned} \quad (2.28)$$

$$\partial_b g(a, b) = -\frac{\pi}{2}\partial_b y - i\,\partial_b \ln H$$

$$= i\xi(a, b) - \frac{1}{2\pi}\int_{-a}^{a} \Theta(a-v)\,\partial_b R(v, b)\,dv \tag{2.29}$$

To obtain $\partial_a g(a, b)$ in the form (2.28), Eqs. (2.16) and (2.14) have been used.

For calculating all these a and b derivatives we need the derivatives of $R(u, b)$ with respect to a and b. These quantities can be obtained by differentiating the integral equation (2.21) with respect to a and b. This yields

$$\partial_a R(u, b) + \frac{1}{2\pi}\int_{-a}^{a} K(u-v)\,\partial_a R(v, b)\,dv$$

$$= -\frac{1}{2\pi}[K(u-a)\,R(a, b) + K(u+a)\,R(-a, b)] \tag{2.30}$$

$$\partial_b R(u, b) + \frac{1}{2\pi}\int_{-a}^{a} K(u-v)\,\partial_b R(v, b)\,dv = \partial_b \xi(u, b) \tag{2.31}$$

These integral equations have the same structure as (2.21) and thus can be treated in the same way. This method for obtaining the derivatives $\partial_a R$ and $\partial_b R$ has been introduced by Lieb and Wu[5] for the special case $b = 0$. It can be used to calculate the free energy $F(h, y)$ and its Legendre transforms analytically for $\Delta < -1$ and $a = \pi$ (see Section 3) and to compute these quantities numerically for all values of Δ provided that a is finite. A second analytically solvable (but rather trivial) case occurs for $a = 0$, i.e., $y = 1$. We will discuss this case in Section 5.

3. ANALYTICAL RESULTS FOR $\Delta < -1$

Here we use the method sketched in Section 2 to calculate exact expressions for the free energies $F(h, y)$, $F(x, y)$, and $F(h, v)$ for $\Delta < -1$ and $a = \pi$. As a first step we solve the integral equation (2.21) and its derivatives with respect to a and b, (2.30) and (2.31), by Fourier analysis. Using these results, we calculate the parameters $h(a, b)$, $y(a, b)$, and $F(h, y)$ as well as their a and b derivatives all for $a = \pi$. Legendre transformation then gives $F(x, y)$ and $F(h, v)$. In this section we present the results. Technical details can be found in Appendices D and E.

For $\Delta < -1$ the kernel $K(u-v)$ and the inhomogeneity $\xi(u, b)$ of the integral equation (2.21) both are 2π-periodic (see Table I). Therefore it is

possible to solve (2.21) by Fourier analysis, provided that $a = \pi$. Hence, we can expand the solution $R_0(u, b)$ of (2.21) in a Fourier series:

$$R_0(u, b) = \sum_{n=-\infty}^{\infty} \hat{R}_n e^{-inu} \tag{3.1}$$

where the coefficients $\hat{R}_n$ are defined by

$$\hat{R}_n = \frac{1}{2\pi} \int_{-\pi}^{\pi} du\, R_0(u, b) e^{inu} \tag{3.2}$$

Note that the Fourier coefficients $\hat{R}_n$ depend on the parameter b. Expressions similar to (3.1) can of course be written down for the functions $\xi(u, b)$ and $K(u-v)$. After a transformation $z = e^{iu}$ (for $n \geqslant 0$) or $z = e^{-iu}$ (for $n < 0$), the Fourier coefficients of $K(u-v)$ and $\xi(u, b)$ can be calculated directly with the help of the residue theorem. We obtain

$$\hat{K}_n = e^{-2\lambda |n|} \tag{3.3}$$

$$\hat{\xi}_n = e^{-\lambda |n| + bn}, \qquad -\lambda < b < \lambda \tag{3.4}$$

Consequently the Fourier coefficients of $R_0(u, b)$ can be calculated as

$$\hat{R}_n = \frac{\hat{\xi}_n}{1 + \hat{K}_n} = \frac{e^{bn}}{2 \cosh \lambda n}, \qquad -\lambda < b < \lambda \tag{3.5}$$

By insertion of the coefficients (3.5) into (3.1), we can write the distribution function $R_0(u, b)$ as

$$R_0(u, b) = \frac{1}{2} + \sum_{n=1}^{\infty} \frac{\cos n(u + ib)}{\cosh n\lambda} \tag{3.6}$$

Below we shall repeatedly need the values of R_0 for $u = \pi$ and $u = -\pi$, which follow directly from this result:

$$R_0(\pi, b) = R_0(-\pi, b) = \frac{1}{2} + \sum_{n=1}^{\infty} (-1)^n \frac{\cosh bn}{\cosh \lambda n} \tag{3.7}$$

Note that the result (3.6) for $R_0(u, b)$ has an extremely simple form: It is the straightforward analytical continuation of a result obtained by Yang and Yang[14] for the quantum Heisenberg chain, where $b = 0$.

Next we calculate the dipole energy h and the polarization y from the generalized normalization (2.22) for $a = \pi$. We deal with the two terms on

the right of (2.22) separately: The function p^0 (see Table I) for $u=\pi$ can be written as

$$p^0(\pi, b)=\pi+i\left[\ln\left(\frac{1+e^{-\lambda-b}}{1+e^{-\lambda+b}}\right)+b\right]$$

The imaginary part of $p^0(\pi, b)$ is then expanded in a Taylor series. In the second contribution we express the function Θ in terms of a complex logarithm in order to obtain integrals of the form given in Appendix E. Using Appendix E, (E.2), with $A=\exp(-2\lambda)$, $B=\exp(2\lambda)$, and $C=2\lambda$, we obtain

$$\frac{\pi}{2}-i\sum_{n=1}^{\infty}\frac{(-1)^n}{n}(1-e^{-2\lambda n})\frac{\sinh bn}{\cosh \lambda n}$$

Combination of these two contributions yields the value of $g(a, b)$ for $a=\pi$:

$$g(\pi, b)=\frac{\pi}{2}+i\left[b+2\sum_{n=1}^{\infty}\frac{(-1)^n}{n}\frac{\sinh bn}{\cosh \lambda n}\right] \tag{3.8}$$

Comparing this result with Eq. (2.22), the generalized normalization, one can directly read off that $y=0$, as expected (see Section 2), while

$$\ln H=2\beta h=-b-2\sum_{n=1}^{\infty}\frac{(-1)^n}{n}\frac{\sinh bn}{\cosh \lambda n} \tag{3.9}$$

Thus, h depends on λ and on b. Recall that (for fixed λ) b can take all values in the interval $-\lambda<b<\lambda$. Using an identity derived by Lieb and Wu,[5] one can rewrite Eq. (3.9) in the following form:

$$\ln H=-2\left\{\ln\left(\frac{\cosh \frac{1}{2}(\lambda+b)}{\cosh \frac{1}{2}(\lambda-b)}\right)-\frac{1}{2}b-\sum_{n=1}^{\infty}\frac{(-1)^n e^{-2n\lambda}\sinh bn}{n\cosh \lambda n}\right\} \tag{3.10}$$

This expression for $\ln H$ converges faster than the first one and is therefore better suited for numerical calculations. It is also possible to rewrite Eq. (3.9) in terms of the Jacobian elliptic function *nd*.[5] In this form it can easily be expanded for small values of λ.

Using these results for R_0 and $\ln H$, we are now able to calculate the free energy $F(h, y)$ from Eq. (2.23). The calculation is straightforward but rather technical. For this reason we prefer to present the details in Appendix D. Here we simply give the results. First we observe that

$-\beta F(h, y)$ is either equal to $\ln \Lambda_R$ or to $\ln \Lambda_L$, whichever is largest. The crossover from $\ln \Lambda_R$ to $\ln \Lambda_L$ occurs at $b = \phi_0$.

$$-\beta F(h, y=0) = \max_{R,L} (\ln \Lambda_R, \ln \Lambda_L)$$

$$= \begin{cases} \ln \Lambda_R & \text{for} \quad -\lambda < b < \phi_0 \\ \ln \Lambda_R = \ln \Lambda_L & \text{for} \quad b = \phi_0 \\ \ln \Lambda_L & \text{for} \quad \phi_0 < b < \lambda \end{cases}$$

One finds that, although both $\ln \Lambda_R$ and $\ln \Lambda_L$ have a kink at $b = \phi_0$, the *maximum* of both (i.e., the free energy) is an analytical function of b (namely a *constant*) even at $b = \phi_0$:

$$-\beta F(h, y=0) = \frac{1}{2} \ln \eta + \frac{1}{2} (\lambda - \phi_0) + \sum_{n=1}^{\infty} \frac{e^{-\lambda n} \sinh(\lambda - \phi_0) n}{n \cosh \lambda n} \tag{3.11}$$

The interpretation of the fact that $F(h, y=0)$ is constant as a function of b will be given at the end of this section.

To calculate the Legendre transforms $F(x, y)$ and $F(h, v)$ [defined in Eqs. (1.8), (1.10)], we use the method sketched in Section 2. The derivatives of the distribution function $(\partial_a R)_0 (u, b)$ and $(\partial_b R)_0 (u, b)$ can be obtained by Fourier analysis of, respectively, Eq. (2.30) or Eq. (2.31) for $a = \pi$. The procedure here is completely analogous to the solution of the integral equation (2.21) itself. The results are

$$(\partial_a R)_0 (u, b) = -R_0(\pi, b) \left[\frac{1}{2} + \sum_{n=0}^{\infty} (-1)^n \frac{e^{-\lambda n} \cos nu}{\cosh \lambda n} \right] \tag{3.12}$$

with the Fourier coefficients

$$\overline{(\partial_a R)}_n = -R_0(\pi, b)(-1)^n \frac{e^{-\lambda |n|}}{2 \cosh \lambda n} \tag{3.13}$$

and

$$(\partial_b R)_0 (u, b) = -i \sum_{n=1}^{\infty} \frac{n \sin n(u + ib)}{\cosh \lambda n} \tag{3.14}$$

with the Fourier coefficients

$$\overline{(\partial_b R)}_n = \frac{n e^{bn}}{2 \cosh \lambda n} = n \hat{R}_n \tag{3.15}$$

Somewhat surprisingly, $(\partial_b R)_0$ is equal to the derivative with respect to b of $R_0(u, b)$ given in Eq. (3.6). Hence the derivative with respect to b and the limit $a \to \pi$ can be interchanged.

Using these results for $(\partial_a R)_0$ and $(\partial_b R)_0$, we calculate the derivatives of y and $\ln H$ with respect to a and b. This can be done as follows: Consider Eqs. (2.28) and (2.29) for $a = \pi$. Note that the occurring integrals can be calculated with the help of Appendix E, (E.2), in the same way as in Eq. (2.22) for $a = \pi$. By insertion of $\Theta(2\pi) = 2\pi$ (see Table I), the Fourier series (3.1) for $(\partial_a R)_0 (u, b)$ with coefficients (3.13), and $R_0(\pi)$ of (3.7) into (2.28), we obtain for $\partial_a g(a + ib)$

$$\partial_a g(a + ib)|_{a=\pi, b} = \tfrac{1}{2} R_0(\pi, b) \tag{3.16}$$

Thus, $\partial_a \ln H = 0$ for $a = \pi$ and

$$\partial_a y = -\frac{1}{\pi} R_0(\pi, b) \tag{3.17}$$

It can be shown that the derivative of y with respect to a is negative for all values of b, as expected (see Section 2).

From Eq. (2.29) we obtain the derivatives with respect to b in the same manner, using now the Fourier series (3.1) with coefficients (3.4) for $\xi(\pi, b)$ and with coefficients (3.15) for $(\partial_b R)_0$ and Appendix E, (E.2). The results are $\partial_b y = 0$ and

$$\partial_b \ln H = -2R_0(\pi, b) \tag{3.18}$$

The last result (3.18) shows that $\partial_b \ln H$ is again simply the derivative with respect to b of $\ln H$, (3.9).

The derivatives $\partial_y a$, $\partial_{\ln H} a$, $\partial_y b$, and $\partial_{\ln H} b$ follow then immediately from (2.27):

$$\begin{aligned} \partial_y a &= -\frac{\pi}{R_0(\pi, b)} \\ \partial_{\ln H} a &= 0 \\ \partial_y b &= 0 \\ \partial_{\ln H} b &= \frac{-1}{2R_0(\pi, b)} \end{aligned} \tag{3.19}$$

The only missing ingredients needed for calculation of the Legendre transforms $F(x, y)$ and $F(h, v)$ are the derivatives of $F(h, y)$ with respect to

a and b. These derivatives can be calculated analogously to the free energy $F(h, y)$ itself. Details are given in Appendices D and E. The results are

$$\partial_a(-\beta F(h, y))|_{b,a=\pi} = \frac{1}{\pi} R_0(\pi, b)\left[\frac{1}{2}(\lambda - |\phi_0 - b|) + \sum_{n=1}^{\infty} \frac{(-1)^n \sinh[(\lambda - |\phi_0 - b|)n]}{n \cosh \lambda n}\right] \tag{3.20}$$

$$\partial_b(-\beta F(h, y))|_{b,a=\pi} = 0$$

We can now collect our results and calculate the Legendre transforms $F(h, y)$ and $F(h, v)$ of $F(h, y)$. The polarization $x(a=\pi, b) = 2\partial_{\ln H}(-\beta F(h, y))$ is zero, as can easily be seen from the definition (1.9). Consequently, $F(x=0, y=0)$ is equal to $F(h, y=0)$ in (3.11). The dipole energy $v = (1/2\beta) \ln V$ is obtained from Eq. (1.11),

$$\ln V(a=\pi, b) = \lambda - |\phi_0 - b| + 2 \sum_{n=1}^{\infty} \frac{(-1)^n \sinh[(\lambda - |\phi_0 - b|)n]}{n \cosh \lambda n} \tag{3.21}$$

Note that $\ln V$ has the same form as $\ln H$, (3.9), so that $(-\ln V)$ can also be written in the form (3.10) by replacement of b by $(\lambda - |\phi_0 - b|)$. Since $y=0$, the Legendre transform $F(h, v)$ is also equal to $F(h, y=0)$, (3.11). This concludes the calculation of the free energies $F(x, y)$ and $F(h, v)$.

The result (3.21) represents the first-order term of the expansion of $F(x, y)$ [or $F(h, y)$] for small values of y. To obtain higher orders one would have to calculate higher derivatives with respect to a and b. These derivatives can in principle be obtained along the same lines as the first-order derivatives discussed above. Technically, putting $b=0$, i.e., $h=0$, represents a serious simplification, since in this case the derivatives with respect to b do not occur and, moreover, all imaginary parts which are usually present are equal to zero. For this special case the expansion of $F(h, y)$ has been carried out up to third order by Lieb and Wu.[5] These authors find that the second-order term vanishes, whereas the third-order term contributes to $F(h, y)$. We expect the same behavior for $b \neq 0$, for, in general, $b=0$ is not a special point in the phase diagram, i.e., the physical situation for $b=0$ and $b \neq 0$ is precisely the same. A rigorous proof of this expectation is lacking.

We emphasize that the final results have already been published almost without derivation by Sutherland *et al.*[4] The derivation of the results in ref. 4 could partly (for the special case $b=0$, or $h=0$) be reconstructed by Lieb and Wu.[5] Our method, which is valid also for $h \neq 0$, is a generalization of the techniques developed by Lieb and Wu. The

main value of the derivation presented here is, first, that it is shown in detail how the results of ref. 4 can be obtained and, second, that in this manner these results are made more easily accessible for numerical analysis. Note that Eq. (3.21) corrects a serious minus-sign error in formula (22) of ref. 4 for $b > \phi_0$: as it stands, this equation is meaningless since it contains a divergent series.

We add a few remarks. First recall that the calculation in this section is valid for all values of b in the interval $-\lambda < b < \lambda$. Because of the symmetry of the model (see Section 2) the free energy can be obtained in the entire (h, v) plane from the result in the region $v \geqslant |h|$. From Eqs. (3.9) and (3.21) one easily shows that this region corresponds to b values in the interval $-\frac{1}{2}(\lambda - \phi_0) \leqslant b \leqslant \frac{1}{2}(\lambda + \phi_0)$, which is included in $-\lambda < b < \lambda$. Next we comment on the shape and geometrical interpretation of the free energies $F(x, y)$ and $F(h, v)$. The exact calculation shows that $F(x, y)$ has a conical singularity in the point $(0, 0)$. This can be seen as follows. The x and y derivatives at this point, which are proportional to $\ln H$, (3.9), and $\ln V$, (3.21), respectively (see Section 2), are different for different values of $b \in [-\frac{1}{2}(\lambda - \phi_0), \frac{1}{2}(\lambda + \phi_0)]$, i.e., for different directions in the (x, y) plane. This implies that one observes a jump in the derivative of $F(x, y)$ if one crosses the origin along some straight line $y = kx$. The symmetry $F(x, y) = F(-x, -y)$ then shows that (for a fixed value of k) the jump is symmetric with respect to the vertical, i.e., F axis. Thus, $F(x, y)$ does not have a unique tangent plane at the point $(0, 0)$. The conical singularity of $F(x, y)$ manifests itself in the shape of $F(h, v)$ as follows. The *point* $(x, y) = (0, 0)$ corresponds to a *region* in the (h, v) plane the boundary of which varies with λ. For fixed λ it is parametrized by b through Eqs. (3.9) and (3.21). For values of h and v within this region the function $F(h, v)$ attains the constant value (3.11). The constancy of $F(h, v)$ follows directly from the fact that its h and v derivatives (i.e., x and y) vanish. We will come back to this behavior in a subsequent article.[10]

4. ANALYTICAL RESULTS FOR $-1 < \Delta < 1$ AND $\Delta = -1$

Next we consider the free energies $F(x, y)$ and $F(h, v)$ as a function of the polarizations x and y or the dipole energies h and v. To obtain $F(x, y)$ and $F(h, v)$ for small values of their arguments, it suffices to solve the integral equation (2.14) asymptotically for large a. This will be done in several steps. First we solve (2.14) for $a = \infty$, where the solution can be found by Fourier transformation. Results for large but finite a can then be obtained by expanding about the solution for $a = \infty$. The logic of this section is as follows: for given (a, b) we calculate the three parameters $h(a, b)$, $y(a, b)$, and $F(h, y)$. Legendre transformations then give $F(x, y)$

and $F(h, v)$. In this section we sketch the calculation and present the results. Technical details are contained in Appendices A–C.

We start with the analytically soluble case $a = \infty$. Here the integral equation (2.14) can be solved by Fourier transformation. For our purposes it is convenient to introduce a slightly modified definition of the Fourier transform, namely

$$\hat{R}(t) = \frac{1}{2\pi} \int_{-\infty + ib}^{\infty + ib} d\alpha \, e^{i\alpha t} R(\alpha) \tag{4.1}$$

The inverse transform is then given by

$$R(\alpha) = \int_{-\infty}^{\infty} dt \, e^{-i\alpha t} \hat{R}(t) \tag{4.2}$$

With these definitions, the solution of (2.14) for $a = \infty$ is easily found as

$$\hat{R}_0((t) = \frac{\hat{\xi}(t)}{1 + \hat{K}(t)} \tag{4.3}$$

The inverse transform $R(\alpha)$ of $\hat{R}(t)$ can also be calculated explicitly. The results are given in Table II.

We add several remarks. First, note that the analytical form of the solution changes at $|b| = \mu$ if $-1 < \Delta < 1$. This change corresponds to a transition from zero polarization ($y = 0$) for $|b| < \mu$ to maximal polarization for all $|b| > \mu$. A similar transition occurs at $|b| = \frac{1}{2}$ if $\Delta = -1$. As a second remark, we observe that the solution in Table II, which is valid for *complex* α, is the analytic continuation of the result for real α given by Yang and Yang.[14]

The next step is the calculation of the polarization y and the dipole energy h from the (generalized) normalization equation (2.18). As may be seen from Eq. (2.19), y and h are determined by the real and imaginary parts of $g(\infty + ib)$, respectively. From (2.18) it is clear that $g(\infty + ib)$ can be expressed in terms of $p^0(\infty + ib)$, $\Theta(\infty)$, and $\hat{R}(0)$. These quantities are given in Table III for the various values of Δ.

Using the results of Table III, one finds that $g(\infty + ib) = \pi/2$ both for $-1 < \Delta < 1$ and $\Delta = -1$, so that [see Eq. (2.19)] $y = 0$ and $h = 0$. The free energy $F(h = 0, y = 0)$ can now be calculated from Eq. (2.20), where $\eta = \exp(\beta\delta)$ [see Eq. (1.2)]. As explained in Section 1, $F(h, y)$ is determined by the right (Λ_R) or left (Λ_L) part of the maximal eigenvalue of the transfer matrix, depending on which is largest. The crossover from Λ_R to

Table II. Explicit Expressions for the Functions $K(\alpha-\beta)$, $\xi(\alpha)$, and $R_0(\alpha)$ and Their Fourier Transforms for $-1<\Delta<1$ and $\Delta=-1$

	$-1<\Delta<1$	$\Delta=-1$
$K(\alpha-\beta)=$	$\dfrac{\sin 2\mu}{\cosh(\alpha-\beta)-\cos 2\mu}$	$\dfrac{2}{1+(\alpha-\beta)^2}$
$\hat{K}(t)=$	$\dfrac{\sinh[(\pi-2\mu)t]}{\sinh(\pi t)}$	$e^{-\lvert t\rvert}$
$\xi(\alpha)=$	$\dfrac{\sin\mu}{\cosh\alpha-\cos\mu}$	$\dfrac{4}{1+4\alpha^2}$
$\hat{\xi}(t)=$	$\begin{cases}\dfrac{\sinh[(\pi-\mu)t]}{\sinh(\pi t)}, & \lvert b\rvert<\mu\\ 0, & \lvert b\rvert>\mu\end{cases}$	$\begin{cases}e^{-\lvert t\rvert/2}, & \lvert b\rvert<\frac{1}{2}\\ 0, & \lvert b\rvert>\frac{1}{2}\end{cases}$
$R_0(\alpha)=$	$\begin{cases}\dfrac{\pi/2\mu}{\cosh[(\pi/2\mu)\alpha]}, & \lvert b\rvert<\mu\\ 0, & \lvert b\rvert>\mu\end{cases}$	$\begin{cases}\dfrac{\pi}{\cosh(\pi\alpha)}, & \lvert b\rvert<\frac{1}{2}\\ 0, & \lvert b\rvert>\frac{1}{2}\end{cases}$
$\hat{R}_0(t)=$	$\begin{cases}\dfrac{1}{2\cosh(\mu t)}, & \lvert b\rvert<\mu\\ 0, & \lvert b\rvert>\mu\end{cases}$	$\begin{cases}\dfrac{1}{2\cosh(t/2)}, & \lvert b\rvert<\frac{1}{2}\\ 0, & \lvert b\rvert>\frac{1}{2}\end{cases}$

Table III. Explicit Results for the Asymptotic Values of p^0 and Θ and for the Fourier Transform $\hat{R}_0(0)$

	$-1<\Delta<1$	$\Delta=-1$
$p^0(\infty+ib)$	$\pi-\mu$	π
$\Theta(\infty)$	$\pi-2\mu$	π
$\hat{R}_0(0)$	$\frac{1}{2}$	$\frac{1}{2}$

Δ_L by definition takes place at $b=\phi_0$ (see Table I), where the function $\Phi(\alpha)$ has a singularity. One finds

$$-\beta F(h=0,\ y=0)$$
$$=\begin{cases}\dfrac{1}{2}\ln\eta+\dfrac{1}{2\pi}\displaystyle\int_{-\infty+ib}^{\infty+ib}\Phi^{R}(\alpha)\,R_0(\alpha)\,d\alpha & \text{for}\quad -b_0<b\leqslant\phi_0\\[2ex] -\dfrac{1}{2}\ln\eta+\dfrac{1}{2\pi}\displaystyle\int_{-\infty+ib}^{\infty+ib}\Phi^{L}(\alpha)\,R_0(\alpha)\,d\alpha & \text{for}\quad \phi_0\leqslant b<b_0\end{cases}\tag{4.4}$$

Here $b_0=\mu$ if $-1<\Delta<1$ and $b_0=\frac{1}{2}$ for $\Delta=-1$. For α we use the parametrization $\alpha=u+ib$ with u and b real. The integrals in (4.4) can be calculated using the residue theorem. Details can be found in Appendices A and B, respectively.

The resulting expressions for $F(h=0,\ y=0)$ are

$$-\beta F(h=0,\ y=0)$$
$$=\frac{1}{2}\ln\eta+\frac{1}{8\mu}\int_{-\infty}^{\infty}\ln\left(\frac{\cosh u-\cos(2\mu-\phi_0)}{\cosh u-\cos\phi_0}\right)\frac{1}{\cosh(\pi u/2\mu)}\,du,$$
$$-1<\Delta<1\tag{4.5}$$

$$-\beta F(h=0,\ y=0)$$
$$=\frac{1}{2}\ln\eta+\ln\left(\frac{\Gamma(1+1/2(\eta+1))\,\Gamma(1/2-1/2(\eta+1))}{\Gamma(1/2+1/2(\eta+1))\,\Gamma(1-1/2(\eta+1))}\right),$$
$$\Delta=-1\tag{4.6}$$

Note that $F(h=0,\ y=0)$ in (4.5) and (4.6) does not depend on the parameter b. The physical explanation for this result will become clear soon. To our knowledge the integral occurring in (4.5) cannot be expressed in a simple way in terms of elementary functions. Note that (4.5) reduces to (4.6) in the limit $\Delta\to-1$ from above. Similarly, one finds that the previous result (3.11) reduces to (4.6) in the limit $\Delta\to-1$ from below.

To calculate the Legendre transforms $F(x,\ y)$ and $F(h,\ v)$ [defined in Eqs. (1.8), (1.10)] we need an expansion of $F(h,\ y)$ in the neighborhood of $(h,\ y)=(0,\ 0)$. Since we found above that $y=0$ and $h=0$ for $a=\infty$, it is clear that small h and y correspond to *large* but finite values of a. An asymptotic study of $F(h,\ y)$ for large a (or small $h,\ y$) is carried out in Appendix C. The method used there is a generalization of the techniques developed by Yang and Yang for the XXZ-Heisenberg chain.[14] The result is

$$-\beta F(h,\ y)=-\beta F(h=0,\ y=0)$$
$$-\frac{\cos(s\phi_0)}{4r}\left[r^2y^2-(\ln H)^2\right]+\frac{1}{2}\sin(s\phi_0)\,y\ln H\tag{4.7}$$

where $s = \pi/2\mu$ and $r = \pi - \mu$ if $-1 < \Delta < 1$ and $s = r = \pi$ for $\Delta = -1$. From this result it directly follows (see Appendix C) that the point $(h, y) = (0, 0)$ corresponds to $x = 0$ and $v = 0$. As a consequence, one has that all three free energies $F(h = 0, y = 0)$, $F(x = 0, y = 0)$, and $F(h = 0, v = 0)$ are identical and equal to (4.5), (4.6).

The expansions of $F(x, y)$ for small x and y of $F(h, v)$ for small h and v can also easily be calculated from (4.7). We obtain

$$-\beta F(x, y) = -\beta F(x = 0, y = 0) - \frac{r}{4\cos(s\phi_0)}\left[x^2 + y^2 - 2xy\sin(s\phi_0)\right] \tag{4.8}$$

and

$$-\beta F(h, v) = -\beta F(h = 0, v = 0) + \frac{1}{4r\cos(s\phi_0)}\left[(\ln V)^2 + (\ln H)^2 + 2\ln V \ln H \sin(s\phi_0)\right] \tag{4.9}$$

Part of these results can also be found in ref. 4, albeit almost without derivation. The explicit expression (4.6) for $F(h = 0, y = 0)$ in the case $\Delta = -1$ is a new result for $b \neq 0$. Lieb and Wu[5] give the same expression for $b = 0$. Using ref. 15, formula 44.8.4, it can be shown that this result is equivalent to Eq. (17) derived by Sutherland *et al.*[4] For numerical applications Eq. (4.6) has great advantages over the rather slowly converging series representation of ref. 4. From (4.7)–(4.9) we see that all three free energies have the form of a paraboloid for small parameters (h, y, x, v). The result differs markedly from the behavior of the free energies found for $\Delta < -1$ (see above).

5. ANALYTICAL RESULTS FOR $a = 0$ AND ALL VALUES OF Δ

Finally, we show which results can be obtained analytically for $a = 0$. We use the method explained in the last part of Section 2 without specifying the functions ξ, K, p^0, Θ, and $\Phi^{R,L}$, which are different for $\Delta < -1$, $\Delta = -1$, and $-1 < \Delta < 1$ (see Table I). For $b \neq \phi_0$ the integrands in Eqs. (2.21)–(2.23) are analytical functions, so that the integrals in these equations vanish for $a = 0$. We obtain from Eq. (2.21) for the distribution function

$$R(u, b) = \xi(u, b)$$

from the generalized normalization (2.22), $y=1$, and $\ln H = -\mathrm{Im}(p^0(0,b))$; and for the free energy $F(h, y)$, provided that $b \neq \phi_0$ (i.e., $\ln H \neq -\ln \eta$),

$$-\beta F(h, y=1) = \begin{cases} \frac{1}{2}(\ln \eta + \ln H), & \ln H > -\ln \eta \\ -\frac{1}{2}(\ln \eta + \ln H), & \ln H < -\ln \eta \end{cases} \tag{5.1}$$

The derivatives with respect to a and b of these quantities can be calculated in the same way from Eqs. (2.28), (2.29), and (2.25). By inserting the results into Eqs. (2.27) and (2.24) we obtain for the polarization x, with the help of relation (1.9), the following result:

$$x = \begin{cases} +1, & \ln H > -\ln \eta \\ -1, & \ln H < -\ln \eta \end{cases}$$

and for the dipole energy v ($=\frac{1}{2}kT \ln V$), with the help of relation (1.11),

$$\ln V \equiv \begin{cases} \ln V^{\mathrm{R}} = \Phi^{\mathrm{R}}(0, b) = \ln \dfrac{2\Delta - \eta - H}{1 - \eta H}, & H > \eta^{-1} \\ \ln V^{\mathrm{L}} = \Phi^{\mathrm{L}}(0, b) = \ln \dfrac{2\Delta - \eta^{-1} - H^{-1}}{1 - \eta^{-1} H^{-1}}, & H < \eta^{-1} \end{cases} \tag{5.2}$$

For the last identity we used Eqs. (2.13) and (2.6) to give expressions for the functions Φ^{R} and Φ^{L} in terms of the old variables p^0 without specifying in which interval Δ lies. The Legendre transforms of $F(h, y)$ then follow immediately from Eqs. (1.8) and (1.10), respectively. The results are

$$F(x, y=1) = \begin{cases} F(x=1, y=1) = -\frac{1}{2}\delta, & h > -\frac{1}{2}\delta \\ F(x=-1, y=1) = \frac{1}{2}\delta, & h < -\frac{1}{2}\delta \end{cases} \tag{5.3}$$

and

$$F(h, v) = \begin{cases} -\frac{1}{2}\delta - h - v, & h > -\frac{1}{2}\delta \quad \text{and} \quad v > v^{\mathrm{R}} \\ +\frac{1}{2}\delta + h - v, & h < -\frac{1}{2}\delta \quad \text{and} \quad v > v^{\mathrm{L}} \end{cases} \tag{5.4}$$

These results can be explained as follows. For $y=1$ there are two possible ordered states of the model, one with $x=1$, where the model is completely frozen in at vertex 1, and one with $x=-1$, where it is completely frozen in at vertex 4. For each of these states the free energy per lattice site $F(x, y)$ naturally takes the constant value of the corresponding vertex energy [see Eqs. (5.3) and (1.1)]. The two points $(x, y, F(x, y)) = (\pm 1, 1, \mp\frac{1}{2}\delta)$ correspond to the two planar parts of $F(h, v)$ in (5.4). Their boundaries $(h, v^{\mathrm{R,L}})$ in the (h, v) plane can be obtained from the result (5.2). These boundaries give the critical strengths of the external horizontal and vertical

fields needed to force the intrinsically antiferroelectric models into a state of maximal polarization (or the intrinsically ferroelectric models into a state where the polarization is not frozen in at its maximal value). These boundaries are of course temperature dependent. For increasing temperature they are shifted to greater field strengths. Because of the symmetry of the models the analogous behavior occurs for $y = -1$ and reversed electric fields. Examples of phase diagrams for an intrinsically antiferroelectric model will be shown elsewhere.[10] A phase diagram for an intrinsically ferroelectric model can be found in ref. 5.

The result (5.2) represents the first-order term of the expansion of $F(x, y)$ for small values of $(1-y)$ and $h \neq -\frac{1}{2}\delta$. For the sake of completeness we mention here that this expansion can be extended to higher orders (see ref. 5 for $b=0$, ref. 8 for $b \neq 0$, and ref. 16 for a special model). All authors find that the next nonzero contribution is not of second order in $(1-y)$ as one might expect, but of third order.

For $h = -\frac{1}{2}\delta$ (i.e., $b = \phi_0$) the integrands in Eqs. (2.23) and (2.25) have logarithmic singularities. Thus the integrals have to be treated more carefully. Sutherland *et al.*[4] give an expansion near $y=1$ for $x \neq \pm 1$ containing also the case $x=0$ (i.e., $h = -\frac{1}{2}\delta$). From their result it follows immediately that $\lim_{y \to 1} F(x=0, y) = 0$, while v and $F(h, v)$ diverge logarithmically.

6. SUMMARY AND DISCUSSION

We start with a summary. In this paper we presented the detailed analytical solution of the asymmetric six-vertex model. The concepts which are central to the method of solution of the six-vertex model, such as the transfer matrix method and the Bethe Ansatz, were briefly discussed in Section 2. It was shown how a closed set of equations for the free energy can be obtained. In Section 3 we considered the low-temperature phase of intrinsically antiferroelectric models ($\Delta < -1$) and showed how the free energy $F(h, y)$ could be calculated for general fields h in the limit of zero polarization ($y \to 0$). We also calculated the Legendre transforms $F(h, v)$ and $F(x, y)$ in this limit. As a byproduct, one finds that $F(x, y)$ has a conical singularity in $(x, y) = (0, 0)$, corresponding to a finite region surrounding the origin in the (h, v) plane. Similarly, the free energy for the high-temperature phase of antiferroelectric ($-1 < \Delta < \frac{1}{2}$) or ferroelectric ($\frac{1}{2} < \Delta < 1$) models is discussed in Section 4. One finds that, in this phase, the free energy has a parabolic form near $(x, y) = (0, 0)$, implying that the finite region in the (h, v) plane, present for $\Delta < -1$, has shrunk to a single point $(0, 0)$ for $-1 < \Delta < 1$. Finally, in Section 5, we studied the free energy and its Legendre transforms for the special case of maximal polarization.

A particular feature of the six-vertex model is that the transition to the state of maximal polarization can occur already at *finite* field strengths (h, v).

As stated in the introduction, the main motivation for this work is that the BCSOS model, which is a microscopic model for the equilibrium shape of bcc crystals,[6] can be mapped exactly onto the asymmetric six-vertex model. Therefore, to study the BCSOS model one has to understand the six-vertex model first. A detailed discussion of the relation between the results presented in this paper and the crystal shapes described by the BCSOS model will be given elsewhere.[10] However, it is readily possible to summarize the basic relations between them[6,7]: The free energy $F(h, v)$ in the six-vertex model is interpreted in the BCSOS model as the height of the crystal surface above some (0, 0, 1) reference plane. For $\Delta < -1$, the finite region in the (h, v) plane, corresponding to the conical singularity in $F(x, y)$, can be interpreted as the occurrence of a (0, 0, 1) facet in the BCSOS model at sufficiently low temperatures ($T < T_R$). The absence of the conical singularity for $\Delta > -1$ implies that the (0, 0, 1) facet has vanished, i.e., that the (0, 0, 1) face of the crystal has become rough. The transition temperature T_R at which the facet vanishes can thus be identified as the roughening temperature of that particular facet. Furthermore, the states of maximal polarization, discussed in Section 5, correspond to the (0, 1, 1) facets in the BCSOS crystal. These facets are present at all temperatures, i.e., for all values of the parameter Δ.

From this brief discussion of the relation between the six-vertex model and the BCSOS model it will be clear that many interesting details of the equilibrium crystal shape are still hidden in the equations derived in Section 2 that determine the free energy $F(x, y)$ and hence its Legendre transform $F(h, v)$. Some properties of the equilibrium crystal can still be calculated analytically, but many others require the numerical calculation of $F(h, v)$. Details concerning the numerical and analytical study of the resulting equilibrium crystal shapes are given elsewhere.[10]

APPENDIX A. DETAILS CONCERNING THE ANALYTICAL SOLUTION ($a = \infty$) FOR $-1 < \Delta < 1$

We distinguish the cases $-\mu < b \leqslant \phi_0$ and $\phi_0 \leqslant b < \mu$, which correspond, respectively, to the situation where Λ^R or Λ^L is largest.

A.1. $-\mu < b \leqslant \Phi_0$ ($\Lambda^R \geqslant \Lambda^L$)

In this case we have to calculate the integral

$$I^R \equiv \int_{-\infty + ib}^{\infty + ib} \Phi^R(\alpha)\, R_0(\alpha)\, d\alpha \tag{A.1}$$

where $\Phi^R(\alpha)$ and $R_0(\alpha)$ are given in Tables I and II, respectively. From the explicit expressions for $\Phi^R(\alpha)$ it is clear that the function Φ^R has logarithmic singularities on the imaginary axis at $ib = i(-2\mu + \phi_0 + k2\pi)$ and $ib = i(\phi_0 + k2\pi)$, and the distribution function $R_0(\alpha)$ has poles on the imaginary axis at $ib = i\mu(1 + 2k)$ $(k \in \mathbf{Z})$. The complex α plane is sketched in Fig. 4. Here we indicate the branch cuts due to the singularities in Φ^R as well as the contour of integration chosen to calculate I^R in the case $b < 0$. For $b \geqslant 0$ we choose a contour in the upper half-plane. Note that the closed contour does not contain any poles. We consider the various parts of the contour in Fig. 4 separately. For $A \to \infty$ the integrals $\int_{-A}^{-A+ib} \Phi^R(\alpha)\, R_0(\alpha)\, d\alpha$ and $\int_{A}^{A+ib} \Phi^R(\alpha)\, R_0(\alpha)\, d\alpha$ are equal to zero. [Recall that $R_0(\alpha)$ falls off exponentially for $|\mathrm{Re}(\alpha)| \to \infty$.] Thus we obtain for $-\mu < b < \phi_0$

$$I^R = \int_{-\infty}^{\infty} \Phi^R(u)\, R_0(u)\, du$$

$$= \frac{1}{2} \int_{-\infty}^{\infty} \ln\left(\frac{\cosh u - \cos(2\mu - \phi_0)}{\cosh u - \cos \phi_0} \right) \frac{\pi/2\mu}{\cosh(\pi u/2\mu)}\, du \qquad \text{(A.2)}$$

which leads to the integral representation of $F(h = 0,\ y = 0)$ in (4.5).

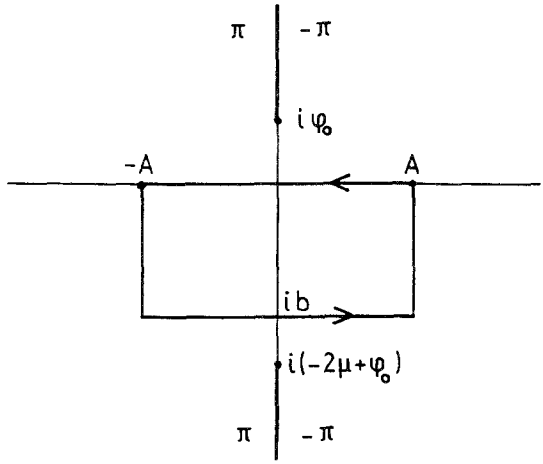

Fig. 4. Logarithmic singularities, branch cuts, and contour of integration in the complex α plane for $b < 0$. The values of the argument of the complex logarithm are indicated on either side of the two cuts.

A.2. $\phi_0 < b < \mu$ ($\Lambda^L > \Lambda^R$)

Here we have to calculate the integral

$$I^L \equiv \int_{-\infty+ib}^{\infty+ib} \Phi^L(\alpha)\, R_0(\alpha)\, d\alpha \tag{A.3}$$

with Φ^L given in Table I and R_0 given in Table II. In this case the function Φ^L has logarithmic singularities on the imaginary axis at $ib = i(2\mu + \phi_0 + k2\pi)$ and $ib = i(\phi_0 + k2\pi)$ ($k \in \mathbf{Z}$). The corresponding branch cuts and the chosen contour of integration are indicated in Fig. 5. The closed contour does not surround any poles. Hence the integral over the chosen contour is equal to zero. For $A \to \infty$ and $\varepsilon \to 0$ the only non-vanishing contributions are I^L, the integrals over the positive and negative real axis, over C_1 and over C_2 (see Fig. 5). Combining all results, one finds

$$I^L = \frac{1}{2}\int_{-\infty}^{\infty} \ln\left(\frac{\cosh u - \cos(2\mu + \phi_0)}{\cosh u - \cos\phi_0}\right) \frac{\pi/2\mu}{\cosh[(\pi/2\mu)u]}\, du$$
$$- 2\pi \ln\left(\frac{\cos(\pi\phi_0/2\mu)}{1 + \sin(\pi\phi_0/2\mu)}\right) \tag{A.4}$$

The second term arises from the contribution due to C_1 and C_2. For physical reasons (see below) (4.4) must lead to the same result for the cases R and L, and thus I^L must be equal to $(I^R + 2\pi \ln \eta)$. This has been checked only numerically.

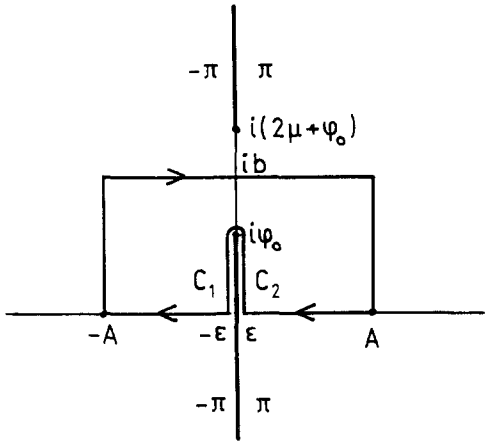

Fig. 5. Logarithmic singularities, branch cuts and contour of integration in the complex α plane for $\phi_0 < b < \mu$. The values of the argument of the complex logarithm are indicated on each side of the two cuts.

APPENDIX B. DETAILS CONCERNING THE ANALYTICAL SOLUTION ($a=\infty$) FOR $\Delta=-1$

The case $\Delta=-1$ can be handled in the same manner as $-1<\Delta<1$. Here we distinguish the parameter intervals $-\frac{1}{2}<b\leqslant\phi_0$ and $\phi_0<b<\frac{1}{2}$.

B.1. $-\frac{1}{2}<b\leqslant\Phi_0$ ($\Lambda^R\geqslant\Lambda^L$)

The calculations proceed along the same lines as those sketched in Appendix A.1. Singularities of Φ^R are now $ib=i\phi_0$ and $ib=i(-1+\phi_0)$ on the imaginary axis; the distribution function $R_0(\alpha)$ has poles at $ib=i(\frac{1}{2}+k)$ ($k\in\mathbf{Z}$) on the imaginary axis. Apart from the different values of the singularities, the situation in the complex α plane is the same as in Fig. 4. Instead of the previous result (A.2), one obtains in this case ($\alpha=u+ib$)

$$
\begin{aligned}
I^R &\equiv \int_{-\infty+ib}^{\infty+ib} \Phi^R(\alpha)\, R_0(\alpha)\, d\alpha = \int_{-\infty}^{\infty} \Phi^R(u)\, R_0(u)\, du \\
&= \frac{1}{2}\int_{-\infty}^{\infty} \ln\left(\frac{(1-\phi_0)^2+u^2}{\phi_0^2+u^2}\right)\frac{\pi}{\cosh \pi u}\, du \\
&= 2\pi \ln\left(\frac{\Gamma((5-2\phi_0)/4)\,\Gamma((1+2\phi_0)/4)}{\Gamma((3-2\phi_0)/4)\,\Gamma((3+2\phi_0)/4)}\right)
\end{aligned}
\tag{B.1}
$$

In the last step we used ref. 17, formula 4.373.1. By inserting (B.1) in combination with the relation between ϕ_0 and η (see Table I) into Eq. (4.4) for $-b_0<b\leqslant\phi_0$ for the free energy $F(h, y)$, one obtains the result given in Eq. (4.6).

B.2. $\Phi_0<b<\frac{1}{2}$ ($\Lambda^L>\Lambda^R$)

The calculations are analogous to those presented in Appendix A.2. The singularities of Φ^L are now given by $ib=i(1+\phi_0)$ and $ib=i\phi_0$, both on the imaginary axis. Here, apart from the values of the singularities, the situation in the complex α plane is the same as in Fig. 5. Instead of Eq. (A.4), we find in this case

$$
\begin{aligned}
&I^L \int_{-\infty+ib}^{\infty+ib} \Phi^L(\alpha)\, R_0(\alpha)\, d\alpha \\
&= 2\pi\left[\ln\left(\frac{\Gamma((5+2\phi_0)/4)\,\Gamma((1+2\phi_0)/4)}{\Gamma((3+2\phi_0)/4)\;\Gamma((3+2\phi_0)/4)}\right) - \ln\left(\frac{\cos \pi\phi_0}{1+\sin \pi\phi_0}\right)\right]
\end{aligned}
\tag{B.2}
$$

The second term arises from the contribution due to C_1 and C_2 (see Fig. 5). Using the relation between ϕ_0 and η (Table I) and ref. 18, formulas 6.1.15 and 6.1.17, we can write this result as

$$I^{\mathrm{L}} = 2\pi \left[\ln \left(\frac{\Gamma((5-2\phi_0)/4)\,\Gamma((1+2\phi_0)/4)}{\Gamma((3-2\phi_0)/4)\,\Gamma((3+2\phi_0)/4)} \right) + \ln \eta \right] \tag{B.3}$$

Insertion of (B.3) into Eq. (4.4) for $-b_0 < b \leqslant \phi_0$ yields precisely the *same* result for the free energy as was found in Appendix B.1. This was to be expected since both results describe the same physical situation (see above).

APPENDIX C. CALCULATION OF $F(h, y)$ NEAR $(h, y) = (0, 0)$

The expression (4.7) for the free energy $F(h, y)$ for small h and y [i.e., for large but finite values of a in (2.20)] is obtained as follows. In Section C.1 we show that h, y, and $F(h, y)$ can be expressed in terms of integrals over the tail $\{|u| > a\}$ of the distribution function $R(u+ib)$. Since R falls off very rapidly for large u, this representation is extremely well suited for the calculation of h, y, and $F(h, y)$ if a is large. Next, in Section C.2, we calculate asymptotic expressions for $R(u+ib)$, valid for $|u| > a$ and $a \to \infty$. The results of Sections C.1 and C.2 are then combined in Section C.3 to calculate explicit expressions for $F(h, y)$, valid if h and y are small. Legendre transformation finally yields the related free energies $F(x, y)$ and $F(h, v)$.

C.1. Tail Formalism for h, y, and $F(h, y)$

Consider the integral equation (2.14) for $R(\alpha)$ ($\alpha = u + ib$). Although $R(\alpha)$ is required only on the *finite* interval $-a \leqslant u \leqslant a$, it is evident that the functions $K(\alpha - \beta)$ and $\xi(\alpha)$ are well-defined for *all* α with $-\infty < u < \infty$. Thus we can regard (2.14) as defining $R(u+ib)$ on the entire real u axis. Equation (2.14) can then be rewritten as an integral equation on the real u axis, using a projection operator B defined by

$$BR(\alpha) = \begin{cases} R(\alpha) & \text{for} \quad |u| \leqslant a \\ 0 & \text{for} \quad a < |u| < \infty \end{cases} \tag{C.1}$$

In terms of B one finds from (2.14) that

$$R(\alpha) = \xi(\alpha) - \frac{1}{2\pi} \int_{-\infty + ib}^{\infty + ib} K(\alpha - \beta)\, BR(\beta)\, d\beta \tag{C.2}$$

For simplicity we use the following abbreviation for Eq. (C.2):

$$R = \xi - KBR \tag{C.3}$$

For $a = \infty$ the solution of this equation can then be cast into the form

$$R_0 = BR_0 = (1+K)^{-1}\,\xi \equiv (1+J)\xi \tag{C.4}$$

where we introduced the resolvent operator J. Equation (C.3) can now be written as

$$(1+K)R = \xi + K(1-B)R \tag{C.5}$$

and with the definition $J \equiv -(1+K)^{-1}K$ as

$$R = (1+K)^{-1}\,\xi - J(1-B)R \tag{C.6}$$

The first term on the right is immediately identified as R_0 [see Eq. (C.4)], so that (C.6) reduces to

$$R = R_0 - J(1-B)R \tag{C.7}$$

or, translated back to the integral notation,

$$\begin{aligned} R(\alpha) = R_0(\alpha) &- \frac{1}{2\pi}\int_{a+ib}^{\infty+ib} J(\alpha-\beta)\,R(\beta)\,d\beta \\ &- \frac{1}{2\pi}\int_{-\infty+ib}^{-a+ib} J(\alpha-\beta)\,R(\beta)\,d\beta \end{aligned} \tag{C.8}$$

This is an integral equation for $R(\alpha)$ with $Re(\alpha) = u$ *outside* the interval $(-a, a)$. Next we show that the polarization y and the dipole energy h can be expressed in terms of integrals over the tail of the distribution function $R(\alpha)$. This result follows directly by integrating Eq. (C.2) over the interval $a < u < \infty$:

$$\begin{aligned} \int_{a+ib}^{\infty+ib} d\alpha\, R(\alpha) &= \int_{a+ib}^{\infty+ib} d\alpha\, \xi(\alpha) - \frac{1}{2\pi}\int_{a+ib}^{\infty+ib} d\alpha \int_{-\infty+ib}^{\infty+ib} d\beta\, K(\alpha-\beta)\,BR(\beta) \\ &= p^0(\infty+ib) - p^0(a+ib) \\ &\quad - \frac{1}{2\pi}\int_{-\infty+ib}^{\infty+ib} d\beta\,\Theta(\infty+ib-\beta)\,BR(\beta) \\ &\quad + \frac{1}{2\pi}\int_{-\infty+ib}^{\infty+ib} d\beta\,\Theta(a+ib-\beta)\,BR(\beta) \end{aligned} \tag{C.9}$$

In the last step we used the definition (2.16) of p^0 as an integral over the function ξ and the relation (2.15) between K and Θ. Combination of the second and fourth terms on the right of (C.9) gives $-g(a+ib)$, as can be seen from Eq. (2.18). The first term on the right, $p^0(\infty+ib)$, and $\Theta(\infty+ib-\beta)=\Theta(\infty)$ occurring in the fourth term are known from Table III. Combining all results, one finds

$$\int_{a+ib}^{\infty+ib} d\alpha\, R(\alpha) = p^0(\infty+ib) - g(a+ib) - \frac{1}{2\pi}\Theta(\infty)\int_{-a+ib}^{a+ib} d\beta\, R(\beta)$$

$$= p^0(\infty+ib)\, y + i \ln H \tag{C.10}$$

In the derivation of (C.10) we used definition (2.19) of y and $\ln H$ $(=2\beta h)$ in terms of $g(a+ib)$ and the normalization (2.17) of $R(\alpha)$. Recall that $p^0(\infty+ib)=\pi$ for $\Delta=-1$ and $p^0(\infty+ib)=\pi-\mu$ if $-1<\Delta<1$. The free energy $F(h, y)$ can be expressed in terms of integrals over the tail of $R(\alpha)$, too. To see this, note that the definition (2.20) of $F(h, y)$ can be written as

$$-\beta F(h, y) = \pm\frac{1}{2}(\ln\eta + \ln H) + \frac{1}{2\pi}\int_{-\infty+ib}^{\infty+ib} d\alpha\, \Phi(\alpha)\, BR(\alpha) \tag{C.11}$$

where the $(+)$ sign corresponds to $\Phi=\Phi^{\mathrm{R}}$ and the $(-)$ sign to $\Phi=\Phi^{\mathrm{L}}$ (see Table I). The function BR occurring in the integral on the right satisfies the integral equation

$$BR = R_0 - (1+K)^{-1}(1-B)R \tag{C.12}$$

This follows directly from the integral equation (C.7) for R by writing $(1+K)^{-1}K = 1-(1+K)^{-1}$ and reshuffling the various terms. Insertion of (C.12) into (C.11) yields

$$-\beta F(h, y) = -\beta F(h=0,\, y=0) \pm \frac{1}{2}\ln H$$

$$-\frac{1}{2\pi}\int_{-\infty+ib}^{\infty+ib} d\alpha\, \Phi(\alpha)[(1+K)^{-1}(1-B)R](\alpha) \tag{C.13}$$

Note that the integral in the right-hand side runs only over the tail $\{|u|>a\}$ of the distribution function $R(\alpha)$.

C.2. Asymptotic Expansion of the Distribution Function $R(\alpha)$ for Large a

To obtain an asymptotic expansion for $R(\alpha)$ in the limit $a\to\infty$, we start from the integral equation (C.8) with $Re(\alpha)$ outside the interval

$(-a, a)$. Using the symmetry $R(-\alpha^*) = R^*(\alpha)$, discussed in Section 2, we rewrite (C.8) in the following way:

$$R(\alpha) = R_0(\alpha) - \frac{1}{2\pi}\int_{a+ib}^{\infty+ib} J(\alpha-\beta)\, R(\beta)\, d\beta$$
$$-\frac{1}{2\pi}\int_{a+ib}^{\infty+ib} J(\alpha+\beta^*)\, R^*(\beta)\, d\beta \tag{C.14}$$

Next we transform (α, β) to new variables (σ, τ), defined by

$$\begin{aligned}\sigma &= \sigma_1 + ib \equiv \alpha - a \\ \tau &= \tau_1 + ib \equiv \beta - a\end{aligned} \tag{C.15}$$

In terms of the new distribution function $S(\sigma) \equiv R(\sigma + a) = R(\alpha)$, Eq. (C.14) reads

$$S(\sigma) + \frac{1}{2\pi}\int_{ib}^{\infty+ib} J(\sigma-\tau)\, S(\tau)\, d\tau$$
$$= R_0(\sigma+a) - \frac{1}{2\pi}\int_{ib}^{\infty+ib} J(\sigma+\tau^*+2a)\, S^*(\tau)\, d\tau \tag{C.16}$$

We estimate the order of magnitude (as a function of the parameter a) of the terms in the RHS of (C.16). The *first* term, $R_0(\sigma+a)$, follows from Table II as $R_0(\sigma+a) \sim 2s\zeta e^{-s\sigma_1}$ for $a \to \infty$, where we defined $\zeta = e^{-s(a+ib)}$ with $s = \pi/2\mu$ if $-1 < \Delta < 1$ and $s = \pi$ for $\Delta = -1$. The second term on the right is much smaller than the LHS of (C.16), since $J(a)$ vanishes for $a \to \infty$, as we shall see below. Hence the second term is also much smaller than the first term on the right, and can therefore be considered as a small perturbation.

Since the integral on the right in (C.16) is small compared to all other terms, we can write $S(\sigma)$ as

$$S(\sigma) = \sum_{k=0}^{\infty} S_k(\sigma) \tag{C.17}$$

where the leading term $S_0(\sigma)$ satisfies the integral equation

$$S_0(\sigma) + \frac{1}{2\pi}\int_{ib}^{\infty+ib} J(\sigma-\tau)\, S_0(\tau)\, d\tau = R_0(a+\sigma) \tag{C.18a}$$

while the higher orders are determined by

$$S_k(\sigma) + \frac{1}{2\pi}\int_{ib}^{\infty+ib} J(\sigma-\tau)\, S_k(\tau)\, d\tau$$
$$= \frac{-1}{2\pi}\int_{ib}^{\infty+ib} J(\sigma+\tau^*+2a)\, S_{k-1}^*(\tau)\, d\tau \tag{C.18b}$$

A formal solution of the integral equation (C.18) for $k=0$ can be obtained by expanding $R_0(a+\sigma)$ and $S_0(\sigma)$ in terms of the small parameter $\zeta = e^{-s(a+ib)}$:

$$R_0(a+\sigma) = 2s \sum_{n=0}^{\infty} (-1)^n \zeta^{2n+1} e^{-s(2n+1)\sigma_1} \tag{C.19a}$$

$$S_0(\sigma) = 2s \sum_{n=0}^{\infty} (-1)^n \zeta^{2n+1} T_n(\sigma_1) \tag{C.19b}$$

The coefficients $T_n(\sigma_1)$ of $S_0(\sigma)$ are real functions of the real variable σ_1 and satisfy

$$T_n(\sigma_1) + \frac{1}{2\pi} \int_0^{\infty} J(\sigma_1 - \tau_1)\, T_n(\tau_1)\, d\tau_1 = e^{-(2n+1)s\sigma_1} \tag{C.20}$$

This is an inhomogeneous Wiener–Hopf equation.

Fortunately, Eq. (C.20) occurs in the literature. This integral equation was studied with the *same* kernel $J(\sigma_1 - \tau_1)$ in the context of the XXZ-Heisenberg chain by Yang and Yang,[14] so that we can simply take over their results here. In particular, it is shown in ref. 14 that the integral kernel vanishes asymptotically for large values of its argument, as was anticipated above. One finds that $J(\alpha) \propto a^{-2}$ for $a \to \infty$ if $\Delta = -1$ and $J(a) \propto e^{-2\pi a}$ if $-1 < \Delta < 1$. This justifies the perturbation expansion (C.17), (C.18). The proof that the corrections due to $S_1 + S_2 + \cdots$ are indeed negligibly small can also be found in ref. 14. The basic result in ref. 14 is the expansion of the ground-state energy in the Heisenberg model for small values of the magnetization. Below (see Appendix C.3) we shall use this result to obtain an expansion of the free energy $F(h, y)$ in the six-vertex model for small h and y.

C.3. Explicit Results for the Free Energies $F(h, y)$, $F(x, y)$, and $F(h, v)$

By combining the results from Sections C.1 and C.2 we are now able to calculate explicit asymptotic expressions for the polarization y, the dipole energy h, and the free energy $F(h, y)$. Legendre transformation then gives $F(x, y)$ and $F(h, v)$.

In Section C.1 we showed that y and h, respectively, can be obtained from the real and imaginary parts of the integral over the tail of the distribution function [see Eq. (C.10)]. As was argued in Section C.2, the distribution function $R(\alpha) \equiv S(\sigma)$ can be written as a sum, $S(\sigma) = \sum_k S_k(\sigma)$, with $S_{k+1} \ll S_k$ for $a \to \infty$. The leading contribution to the LHS of (C.10)

is therefore obtained by neglecting corrections due to $S_1 + S_2 + \cdots$, i.e., by taking only S_0 into account:

$$\int_{a+ib}^{\infty+ib} R(\alpha)\, d\alpha \sim \int_{ib}^{\infty+ib} S_0(\sigma)\, d\sigma \qquad (a \to \infty)$$

$$= 2s \sum_{n=0}^{\infty} (-1)^n \zeta^{2n+1} \int_0^{\infty} d\sigma_1 T_n(\sigma_1)$$

$$= 2s \sum_{n=0}^{\infty} (-1)^n \zeta^{2n+1} \tilde{T}_n(0) \tag{C.21}$$

In the last step we introduced $\tilde{T}_n(\omega)$, which is in general related to the coefficients $T_n(\sigma)$ in the series expansion (C.19b) of $S_0(\sigma)$ by

$$\tilde{T}_n(\omega) \equiv \int_0^{\infty} d\sigma_1 e^{i\omega\sigma_1} T_n(\sigma_1) \tag{C.22}$$

Since the perturbation $S_1 + S_2 + \cdots$ introduces corrections of the form ζ^3 if $-1 < \Delta < 1$, or $(\zeta/\ln \zeta)$ if $\Delta = -1$ (see ref. 14), one can neglect all higher orders ($n > 0$) in (C.21). One then obtains [see (C.10)]

$$ry + i \ln H \sim 2s\tilde{T}_0(0)\zeta \qquad (a \to \infty) \tag{C.23}$$

with the abbreviation $r = p^0(\infty + ib)$, or, using the definition of ζ,

$$y \sim \frac{2s}{r} \tilde{T}_0(0) e^{-sa} \cos(sb) \qquad (a \to \infty) \tag{C.24a}$$

$$\ln H \sim -2s\tilde{T}_0(0) e^{-sa} \sin(sb) \qquad (a \to \infty) \tag{C.24b}$$

Note that $\ln H \sim -ry \tan(sb)$ is of the same order of magnitude as y for $a \to \infty$, or $y \to 0$. By inverting the relation (C.23) between ζ and $(y, \ln H)$, one obtains

$$\zeta = (ry + i \ln H)/2s\tilde{T}_0(0) + o(y) \qquad (a \to \infty) \tag{C.25}$$

Thus, ζ is also of order y (or $\ln H$) for $a \to \infty$, or $y \to 0$.

Next we address the calculation of the free energy $F(h, y)$ for small h and y. The method used below is a generalization to models with $b \neq 0$ of a method invented for $b = 0$ by Lieb and Wu.[5] As can be seen from Eq. (C.13), $F(h, y)$ is expressed in terms of an integral over the tail of $R(\alpha)$. It is convenient to rewrite Eq. (C.13) in the form

$$-\beta F(h, y) = -\beta F(0, 0) \pm \frac{1}{2} \ln H - \frac{1}{2\pi} I_D \tag{C.26}$$

where we defined the integral I_D. It is clear from Eq. (C.13) that I_D has two different forms for Φ_R and Φ_L. For simplicity, we drop the indices R or L in the following formal derivation. In operator notation, I_D can be written as

$$I_D = D[(1-B)R] \tag{C.27}$$

where the functional D is defined by

$$D[f] \equiv \int_{-\infty+ib}^{\infty+ib} d\alpha\, \Phi(\alpha)[(1+K)^{-1} f](\alpha) \tag{C.28}$$

The linear *functional* D can be expressed in terms of a *function* $D(\alpha)$ as follows:

$$D[f] = \int_{-\infty+ib}^{\infty+ib} d\alpha\, D(\alpha)\, f(\alpha) \tag{C.29}$$

The function $D(\alpha)$ will be calculated next. From this result the asymptotic expansion for $F(h, v)$ will follow immediately.

Consider the definition (C.28) of D. In an obvious operator notation, (C.28) can be written as $D = \Phi(1+K)^{-1}$, or, because of the symmetry of $(1+K)^{-1}$, $(1+K)\,D = \Phi$, or equivalently

$$D(\alpha) + \frac{1}{2\pi} \int_{-\infty+ib}^{\infty+ib} d\beta\, K(\alpha-\beta)\, D(\beta) = \Phi(\alpha) \tag{C.30}$$

Thus, $D(\alpha)$ satisfies an integral equation of the same form as $R(\alpha)$ in (2.14). Note, however, that the inhomogeneity is different. The form of Eq. (C.30) clearly suggests a solution by Fourier transformation, but unfortunately the Fourier transform (4.1) of the inhomogeneity $\Phi(\alpha)$ is not well-defined (i.e., does not converge). To circumvent this problem, we take the derivative of (C.30) with respect to α, yielding

$$\dot{D}(\alpha) + \frac{1}{2\pi} \int_{-\infty+ib}^{\infty+ib} d\beta\, K(\alpha-\beta)\, \dot{D}(\beta) = \dot{\Phi}(\alpha) \tag{C.31}$$

From this new equation for the derivative of $D(\alpha)$, $\dot{D}(\alpha)$, we *can* calculate the Fourier transform

$$\hat{\dot{D}}(t) = \hat{\dot{\Phi}}(t)/[1+\hat{K}(t)] \tag{C.32}$$

From the inverse transform $\dot{D}(\alpha)$ one then finds $D(\alpha)$ up to an integration constant:

$$D(\alpha) = \int d\alpha\, \dot{D}(\alpha) + \text{const} = \int_{-\infty}^{\infty} dt\, \frac{e^{-i\alpha t}}{-it}\, \hat{\dot{D}}(t) + \text{const} \tag{C.33}$$

The constant can be obtained from the asymptotic behavior of the integral equation (C.30) for $D(\alpha)$:

$$D(\pm\infty) = \Phi(\pm\infty)/[1+\hat{K}(0)] \tag{C.34}$$

In calculating $D(\alpha)$ explicitly we have to distinguish the two possibilities D^{R} and D^{L} corresponding to the different forms Φ^{R} and Φ^{L} for Φ. The results are given in Table IV. To obtain the expressions for $D^{\mathrm{R}}(\alpha)$ and $D^{\mathrm{L}}(\alpha)$ we used ref. 17, Eq. (3.524.23).

Consider again the integral I_D in (C.28). Using the symmetry $R(-\alpha^*) = R^*(\alpha)$, one can combine the contributions coming from both tails into a single integral:

$$I_D = \int_{a+ib}^{\infty+ib} d\alpha [D^{\mathrm{R,L}}(\alpha)\, R(\alpha) + D^{\mathrm{R,L}}(-\alpha^*)\, R^*(\alpha)] \tag{C.35}$$

Table IV. Explicit Results Needed for Calculation of the Function $D(\alpha)$ for $-1<\Delta<1$ and $\Delta=-1$

	$-1<\Delta<1$	$\Delta=-1$
$\dot{\Phi}^{\mathrm{R}}(\alpha)=$	$\dfrac{e^{\alpha}}{e^{\alpha}-e^{-i(2\mu-\phi_0)}}-\dfrac{e^{\alpha}}{e^{\alpha}-e^{i\phi_0}}$	$\dfrac{-i}{1-\phi_0-i\alpha}-\dfrac{i}{\phi_0+i\alpha}$
$\dot{\Phi}^{\mathrm{L}}(\alpha)=$	$\dfrac{e^{\alpha}}{e^{\alpha}-e^{i(2\mu+\phi_0)}}-\dfrac{e^{\alpha}}{e^{\alpha}-e^{i\phi_0}}$	$\dfrac{i}{1+\phi_0+i\alpha}-\dfrac{i}{\phi_0+i\alpha}$
$\hat{\dot{D}}^{\mathrm{R}}(t)=$	$-i\dfrac{e^{t(\mu-\phi_0)}}{2\cosh \mu t}$	$\dfrac{-i}{1+e^{-\lvert t\rvert}}\begin{cases} e^{-\phi_0 t}, & t\geqslant 0 \\ e^{(1-\phi_0)t}, & t<0 \end{cases}$
$\hat{\dot{D}}^{\mathrm{L}}(t)=$	$i\dfrac{e^{-t(\mu+\phi_0)}}{2\cosh \mu t}$	$\dfrac{i}{1+e^{-\lvert t\rvert}}\begin{cases} e^{-(1+\phi_0)t}, & t\geqslant 0 \\ e^{-\phi_0 t}, & t<0 \end{cases}$
$D^{\mathrm{R}}(\alpha)=$	$\ln\left[\cot\left(\dfrac{\pi}{4}\dfrac{\phi_0+i\alpha}{\mu}\right)\right]$	$\ln\left\{\cot\left[\dfrac{\pi}{2}(\phi_0+i\alpha)\right]\right\}$
$\Phi^{\mathrm{R}}(\pm\infty)=$	$\mp i(\pi-\mu)$	$\mp i\pi$
$D^{\mathrm{R}}(\pm\infty)=$	$\mp i\dfrac{\pi}{2}$	$\mp i\dfrac{\pi}{2}$
$D^{\mathrm{L}}(\alpha)=$	$\ln\left[-\cot\left(\dfrac{\pi}{4}\dfrac{\phi_0+i\alpha}{\mu}\right)\right]$	$\ln\left\{-\cot\left[\dfrac{\pi}{2}(\phi_0+i\alpha)\right]\right\}$
$\Phi^{\mathrm{L}}(\pm\infty)=$	$\pm i(\pi-\mu)$	$\pm\pi$
$D^{\mathrm{L}}(\pm\infty)=$	$\pm i\dfrac{\pi}{2}$	$\pm i\dfrac{\pi}{2}$

Here $D^{R,L}(\alpha)$ and $D^{R,L}(-\alpha^*)$, with $\alpha \equiv a + ib + \sigma_1$, can be expanded for large values of a as

$$D^{R,L}(\alpha) \sim \mp i\frac{\pi}{2} + 2\zeta e^{-s\sigma_1 + is\phi_0} + \mathcal{O}(\zeta^3) \tag{C.36a}$$

$$D^{R,L}(-\alpha^*) \sim \pm i\frac{\pi}{2} + 2\zeta^* e^{-s\sigma_1 - is\phi_0} + \mathcal{O}((\zeta^*)^3) \tag{C.36b}$$

This result can now be inserted into (C.35). The contribution of the *leading* terms on the right in (C.36a) and (C.36b) is

$$\pm\pi \int_{ib}^{\infty + ib} d\sigma \, \mathrm{Im}(S(\sigma)) = \pm\pi \ln H \tag{C.37}$$

where we used the relation (C.10) for $\ln H$. The correction terms in (C.36), proportional to $\zeta = e^{-s(a+ib)}$, yield contributions to I_D of order ζ^2, since $R(\alpha) \equiv S(\sigma)$ in (C.35) is also proportional to ζ [see (C.19b)]. Replacing $S(\sigma)$ in (C.35) by $S_0(\sigma)$, which is the dominant contribution for $a \to \infty$, and using the expansion (C.19b) of S_0 in terms of ζ, one finds that

$$I_D \sim \pm\pi \ln H + 4s\tilde{T}_0(is)[\zeta^2 e^{is\phi_0} + (\zeta^*)^2 e^{-is\phi_0}] \qquad (a \to \infty) \tag{C.38}$$

with definition (C.22) for $\tilde{T}_0(i\omega)$.

We can now collect our results. Insertion of (C.38) into the expression (C.26) for the free energy yields in combination with (C.25) for ζ in terms of y and $\ln H$:

$$\begin{aligned} -\beta F(h, y) = &-\beta F(0, 0) - \frac{1}{2\pi s}\frac{\tilde{T}_0(is)}{[\tilde{T}_0(0)]^2}[(ry + i\ln H)^2 e^{is\phi_0} \\ &+ (ry - i\ln H)^2 e^{-is\phi_0}], \qquad (a \to \infty) \end{aligned} \tag{C.39}$$

Fortunately, the prefactor $\{\tilde{T}_0(is)/[\tilde{T}_0(0)]^2\}$ in (C.39) has already been calculated by Yang and Yang[14] in their study of the quantum Heisenberg chain. Its value is equal to $\pi^2/8\mu(\pi - \mu)$ if $-1 < \Delta < 1$ and equal to $\pi/4$ for $\Delta = -1$. After some elementary algebra one finds that Eq. (C.39) for $F(h, y)$ can also be cast into the form (4.7) presented in Section 4.

It is now straightforward to calculate the Legendre transforms $F(x, y)$ and $F(h, v)$ of $F(h, y)$. As shown in Section 2, the polarization x can be expressed in terms of $\ln H$ and y as

$$x = 2\frac{\partial(-\beta F(h, y))}{\partial(\ln H)}\bigg|_y = \frac{\cos(s\phi_0)}{r}\ln H + \sin(s\phi_0)\, y \tag{C.40}$$

(Here we used the abbreviation $r=\pi-\mu$ if $-1<\Delta<1$ or $r=\pi$ for $\Delta=-1$, respectively.) Hence x is equal to zero for $\ln H=0$ and $y=0$. By solving Eq. (C.40) for $\ln H$ and inserting the result into the Legendre transformation $-\beta F(x, y)=-\beta F(h, y)-\frac{1}{2}x \ln H$, we obtain the expansion (4.8) of $F(x, y)$ for small values of x and y.

The expansion of $F(h, v)$ for small h and v can be calculated in an analogous way. First we express $\ln V=2\beta v$ in terms of $\ln H$ and y:

$$\ln V=-2\left.\frac{\partial(-\beta F(h, y))}{\partial y}\right|_h=r\cos(s\phi_0)\, y-\sin(s\phi_0)\ln H \qquad \text{(C.41)}$$

Note that $v=0$ if $(h, y)=(0, 0)$. It is easy to calculate y as a function of $\ln H$ and $\ln V$ from (C.41). Substitution of the result into the Legendre transformation $-\beta F(h, v)=-\beta F(h, y)+\frac{1}{2}y \ln V$ finally yields Eq. (4.9) for the free energy $F(h, v)$.

APPENDIX D. DETAILS CONCERNING THE ANALYTICAL SOLUTION ($a=\pi$) FOR $\Delta<-1$

The structure of this Appendix is as follows. First we consider the free energy $F(h, y)$, which is given by the maximum of $\ln \Lambda_R$ and $\ln \Lambda_L$ (see Section 2). We calculate $\ln \Lambda_R$ and $\ln \Lambda_L$ and compare the two, in order to determine which is the larger one. This is done for the parameter intervals $-\lambda<b\leqslant\phi_0$ and $\phi_0<b<\lambda$ separately. In addition, we calculate the derivatives of $F(h, y)$ with respect to a and b in $y=0$. These derivatives are needed to carry out the Legendre transformation in Section 3.

A general expression for $\ln \Lambda_R$ and $\ln \Lambda_L$ is obtained by insertion of the Fourier expansion (3.1) of the distribution function $R(u, b)$ into Eq. (2.20). The result is

$$\ln \Lambda_{R,L}=\pm\frac{1}{2}(\ln \eta+\ln H)+\frac{1}{2\pi}\sum_{n=-\infty}^{\infty}\hat{R}_n\int_{-\pi}^{\pi}\Phi^{R,L}(u, b)e^{-inu}\,du \qquad \text{(D.1)}$$

This equation is the starting point for our detailed calculations below.

D.1. $-\lambda<b\leqslant\phi_0$

First we consider b in the interval $-\lambda<b\leqslant\phi_0$. We insert the explicit form of $\Phi^R(u, b)$ from Table I into (D.1) and transform to new variables $z=e^{-iu}$ if $n\geqslant 0$ in (D.1) or $z=e^{iu}$ if $n<0$. The advantage of splitting the sum into terms with $n\geqslant 0$ and $n<0$ is that consequently all integrals

occurring in $\ln \Lambda_R$ have the same form. The calculation of integrals of this type is discussed in Appendix E:

$$\ln \Lambda_R = \frac{1}{2}(\ln \eta + \ln H) - \frac{i}{2\pi}\left\{\sum_{n=0}^{\infty} \hat{R}_n \oint_C \left[\ln\left(\frac{z - e^{-2\lambda+\phi_0-b}}{e^{\phi_0-b}-z}\right)+\lambda\right] z^{n-1}\,dz - \sum_{n=1}^{\infty} \hat{R}_{-n} \oint_C \left[\ln\left(\frac{z-e^{-\phi_0+b}}{e^{2\lambda-\phi_0+b}-z}\right)+\lambda\right] z^{n-1}\,dz\right\} \tag{D.2}$$

Here C is a closed contour of integration running counterclockwise along the unit circle $|z| = 1$. Using the results of Appendix E, Table V, row 3, one finds

$$\ln \Lambda_R = \frac{1}{2}(\ln \eta + \ln H) + \frac{1}{2}(\lambda - \phi_0 + b) + \sum_{n=1}^{\infty} \frac{(-1)^n}{n} \frac{\sinh bn}{\cosh \lambda n} + \sum_{n=1}^{\infty} \frac{e^{-\lambda n} \sinh(\lambda - \phi_0)n}{n \cosh \lambda n} \tag{D.3}$$

Inserting $\ln H$, (3.9), into (D.3), we obtain the final result $\ln \Lambda_R = -\beta F(h, y=0)$, (3.11), given in Section 3.

Next we calculate $\ln \Lambda_L$ for b in the same interval and show that for all values of b in this interval, $\ln \Lambda_R$ is greater than $\ln \Lambda_L$. We insert $\Phi^L(u, b)$ from Table I into Eq. (D.1) and apply the same transformations to the unit circle as were discussed above. The integrals on the right can be calculated using Table V, rows 5 and 1, of Appendix E. As a result, one finds

$$\ln \Lambda_L = -\frac{1}{2}(\ln \eta + \ln H) + \frac{i}{2\pi}\left\{\sum_{n=1}^{\infty} \hat{R}_n \oint_C \left[\ln\left(\frac{z - e^{\phi_0-b}}{e^{2\lambda+\phi_0-b}-z}\right)+\lambda\right] z^{n-1}\,dz - \sum_{n=0}^{\infty} \hat{R}_{-n} \oint_C \left[\ln\left(\frac{z-e^{-2\lambda-\phi_0+b}}{e^{-\phi_0+b}-z}\right)+\lambda\right] z^{n-1}\,dz\right\} \tag{D.4}$$

$$= -\frac{1}{2}(\ln \eta + \ln H) + \frac{1}{2}\lambda + \sum_{n=1}^{\infty} \frac{1}{n} e^{(-\lambda-\phi_0)n} \tanh \lambda n + \sum_{n=1}^{\infty} \frac{\sinh bn}{n \cosh \lambda n} \tag{D.5}$$

where C is the same integration path as in (D.2). To show that $\ln \Lambda_L$ is smaller than $\ln \Lambda^R$, we invert the definition of ϕ_0 in terms of η (see Table I) to obtain the following expression for $\ln \eta$:

$$\ln \eta = \phi_0 + 2 \sum_{n=1}^{\infty} \frac{1}{n} e^{-\lambda n} \sinh \phi_0 n \tag{D.6}$$

Next we insert Eq. (D.6) into Eq. (D.5). After some algebra one can show that Eq. (D.5) is equivalent to

$$\ln \Lambda_L - \ln \Lambda_R = -\frac{1}{2}(\phi_0 - b) - \sum_{n=1}^{\infty} \frac{\sinh \phi_0 n - \sinh bn}{n \cosh \lambda n} \tag{D.7}$$

showing that for $-\lambda < b < \phi_0$ the difference between $\ln \Lambda_L$ and $\ln \Lambda_R$ is always negative.

For $b = \phi_0$ we use the results of Table V, rows 2 and 4, to obtain $\ln \Lambda_R = \ln \Lambda_L = -\beta F(h, y = 0)$.

D.2. $\phi_0 < b < \lambda$

In this case the free energy $F(h, y)$ is determined by $\ln \Lambda_L$, as we shall see below. We find again the expression (D.4) for $\ln \Lambda_L$, where the integrals can now be taken from Table V, row 3. Using the result for $\ln H$, (3.9), we find for $\ln \Lambda_L$

$$\ln \Lambda_L = -\frac{1}{2} \ln \eta + \frac{1}{2}(\lambda + \phi_0) + \sum_{n=1}^{\infty} \frac{e^{-\lambda n} \sinh(\lambda + \phi_0) n}{n \cosh \lambda n} \tag{D.8}$$

With the use of Eq. (D.6) for $\ln \eta$ in terms of ϕ_0 one can easily show that (D.8) is equal to the result (3.11) for $-\beta F(h, y = 0)$ presented in Section 3.

Next we calculate $\ln \Lambda_R$ for $\phi_0 < b < \lambda$ and check that $\ln \Lambda_R < \ln \Lambda_L$ for all b in this interval. Combination of Eq. (D.2) and Table V, rows 1 and 5, gives

$$\ln \Lambda_R = \frac{1}{2} \ln \eta + \frac{1}{2}(\lambda - b) + \sum_{n=1}^{\infty} \frac{1}{n} e^{(-\lambda + \phi_0) n} \tanh \lambda n - \sum_{n=1}^{\infty} \frac{\sinh bn}{n \cosh \lambda n} \tag{D.9}$$

From this result one can show with the help of Eq. (D.6) that the difference between $\ln \Lambda_R$ and $\ln \Lambda_L$ is negative for all b in the interval under consideration:

$$\ln \Lambda_R - \ln \Lambda_L = -\frac{1}{2}(b - \phi_0) - \sum_{n=1}^{\infty} \frac{\sinh bn - \sinh \phi_0 n}{n \cosh \lambda n} < 0$$

D.3. Calculation of $\partial_a F(h, y)$ and $\partial_b F(h, y)$ for $y = 0$

To calculate the derivatives $\partial_a F(h, y)$ and $\partial_b F(h, y)$ of the free energy $F(h, y)$, we start from, respectively, Eq. (2.25) and Eq. (2.26) with $a = \pi$. From the above we conclude that the relevant choice for $\Phi(u, b)$ is $\Phi = \Phi^R$ for $-\lambda < b \leqslant \phi_0$ and $\Phi = \Phi^L$ for $\phi_0 < b < \lambda$. We insert the derivatives $(\partial_a R)_0(u, b)$ [see (3.12)] and $(\partial_b R)_0(u, b)$ [see (3.14)] of the distribution

function $R_0(u, b)$ into (2.25) and (2.26). After a transformation $z = e^{iu}$ (or z^{-iu}) we obtain integrals of the same type as in Sections D.1 and D.2, which can be looked up in Table V of Appendix E. In addition, (2.26) contains integrals of the form $\int_{-\pi}^{\pi} \partial_b \Phi(u, b)\, R(u, b)\, du$, which can be reduced to standard integrals of type

$$\oint_C \frac{z^n}{z - A}\, dz$$

The path of integration C is directed counterclockwise along the unit circle.

For the derivative $\partial_a F(h, y)$ one obtains in this way the following result:

$$-\beta\, \partial_a F(h, y) = \pm\frac{1}{2}\, \partial_a \ln H + \frac{1}{\pi} R_0(\pi, b) \left\{ \frac{1}{2} [\lambda \mp (\phi_0 - b)] + \sum_{n=1}^{\infty} \frac{(-1)^n}{n} \frac{\sinh[\lambda \mp (\phi_0 - b)n]}{\cosh \lambda n} \right\} \tag{D.10}$$

With $\partial_a \ln H = 0$ for $a = \pi$ this result is identical to Eq. (3.20) presented in Section 3. Similarly one finds for $\partial_b F(h, y)$

$$-\beta\, \partial_b F(h, y) = \pm\tfrac{1}{2}\, \partial_b \ln H \pm R_0(\pi, b) \tag{D.11}$$

Using the result (3.18) that $\partial_b \ln H = -2R_0(\pi, b)$, we see immediately that $\partial_b F(h, y = 0) = 0$ for all b in the interval $(-\lambda, \lambda)$.

APPENDIX E. SOME TECHNICAL RESULTS FOR $\Delta < -1$ AND $a = \pi$

All integrals occurring in the analytical solution ($a = \pi$) for $\Delta < -1$ (Section 3 and Appendix D) have the same form, namely

$$I(n) = \oint_D \left[\ln\left(\frac{z - A}{B - z}\right) + C \right] z^{n-1}\, dz, \qquad n \geqslant 0 \tag{E.1}$$

The integration path D is the unit circle $|z| = 1$, described counterclockwise. The parameters A, B, and C are real numbers, A and B being positive with $A < B$.

The integrand in (E.1) has logarithmic singularities on the real axis at $z = A$ and $z = B$. For $n = 0$ there occurs an additional pole at $z = 0$. The situation in the complex z plane depends on the values of A and B. A sketch for the example $A < 1 < B$ is drawn in Fig. 6 for $n > 0$ and for $n = 0$. The branch cuts as well as the arguments of the complex logarithm

are the same for all combinations of A and B. The contour of integration, however, is slightly different for the various cases. Here we discuss the example $A<1<B$ in some detail; results for different combinations of A and B are collected in Table V.

We focus on $A<1<B$. As can be seen from Fig. 6, the closed contour does not contain singularities for any value of $n \geqslant 0$. First consider $n>0$. We choose the closed contour illustrated in Fig. 6, involving the unit circle, two paths along the real axis described in opposite directions and on opposite sides of the branch cut, and a small circle around $z=A$ whose radius ε will eventually be made to approach zero. Apart from the sought integral over the unit circle (E.1), in the limit $\varepsilon \to 0$ there are nonvanishing contributions to the contour integral coming from the pieces along the real axis. Their value is, for $n>0$,

$$\lim_{\varepsilon \to 0} \left\{ \int_{-1}^{A-\varepsilon} \left[\ln \left| \frac{x-A}{B-x} \right| + C + i\pi + i\pi \right] x^{n-1}\, dx \right.$$
$$\left. + \int_{A-\varepsilon}^{-1} \left[\ln \left| \frac{x-A}{B-x} \right| + C - i\pi + i\pi \right] x^{n-1}\, dx \right\}$$
$$= \lim_{\varepsilon \to 0} \left\{ -\frac{2\pi i}{n} [(-1)^n - (A-\varepsilon)^n] \right\} = \frac{-2\pi i}{n} [(-1)^n - A^n]$$

This yields the result in row 3 of Table V for $I(n)$ $(n>0)$.

Along similar lines, one finds a contribution $2\pi i \ln A$ for $n=0$, plus an additional contribution coming from the pole at $z=0$. The two integrals over the upper and lower half-circle $|z|=\varepsilon$ (see Fig. 6b) together are equal

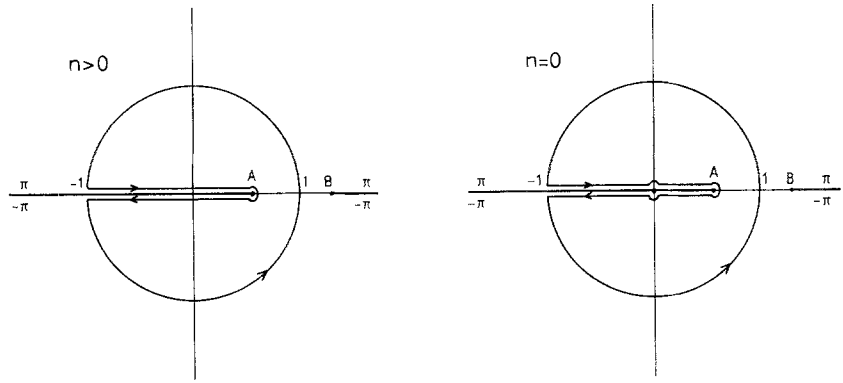

Fig. 6. Branch cuts and contour of integration in the complex z plane for $A<1<B$. The values of the argument of the complex logarithm are indicated on either side of the cuts. (a) $n>0$; (b) $n=0$.

Table V. Results for the Integral (E.1) for Different Combinations of A and B

	$I(n)$, $n>0$	$I(n)$, $n=0$
1. $A<B<1$	$(2\pi i/n)[(-1)^n-1-A^n+B^n]$	$2\pi iC$
2. $A<B=1$	$(2\pi i/n)[(-1)^n-A^n]$	$2\pi iC$
3. $A<1<B$	$(2\pi i/n)[(-1)^n-A^n]$	$2\pi i[C-\ln B]$
4. $A=1<B$	$(2\pi i/n)[(-1)^n-1]$	$2\pi i[C-\ln B]$
5. $1<A<B$	$(2\pi i/n)[(-1)^n-1]$	$2\pi i[C-\ln B+\ln A]$

to $-2\pi i(C-\ln B+\ln A)$. Combination of all terms leads to the result given for $n=0$ in Table V, row 3.

The integrals occurring in Eqs. (2.22), (2.28), and (2.29) for $a=\pi$ have to be handled in a slightly different way: Defining $z=e^{iw}$ with $0\leqslant w\leqslant 2\pi$, we can write the integrand in the same form as in Eq. (E.1). In order to get the right branch of the logarithm, however, in this case we choose the complementary branch cut in the complex z plane, lying on the real axis between A and B with $w=0$ on the upper side of the cut and $w=2\pi$ on the lower side. This leads to a slightly different integration contour $\tilde{D}$. Similar calculations as above yield the following results for $A<1<B$:

$$\oint_{\tilde{D}}\left[\ln\left(\frac{z-A}{B-z}\right)+C\right]z^{n-1}\,dz=\begin{cases}(2\pi i/n)[1-A^n], & n>0\\ 2\pi i[C-\ln B+i\pi], & n=0\end{cases}\qquad\text{(E.2)}$$

ACKNOWLEDGMENTS

It is a pleasure to thank the Institute for Theoretical Physics of the State University at Utrecht for its hospitality during the years 1986–1990. In particular I wish to thank Prof. H. van Beijeren for his support.

REFERENCES

1. J. C. Slater, *J. Chem. Phys.* **9**:16 (1941).
2. E. H. Lieb, *Phys. Rev.* **162**:162 (1967).
3. B. Sutherland, *Phys. Rev. Lett.* **19**:103 (1967).
4. C. P. Yang, *Phys. Rev. Lett.* **19**:586 (1967); B. Sutherland, C. N. Yang, and C. P. Yang, *Phys. Rev. Lett.* **19**:588 (1967).
5. E. H. Lieb and F. Y. Wu, in *Phase Transitions and Critical Phenomena*, Vol. 1, C. Domb and N. S. Green, eds. (Academic Press, London, 1972).
6. H. van Beijeren, *Phys. Rev. Lett.* **38**:993 (1977).
7. C. Jayaprakash, W. F. Saam, and S. Teitel, *Phys. Rev. Lett.* **50**:2017 (1983).
8. C. Jayaprakash and W. F. Saam, *Phys. Rev. B* **30**:3917 (1984).
9. I. M. Nolden, Thesis, Rijksuniversiteit te Utrecht (1990).
10. I. M. Nolden and H. van Beijeren, to be published.

11. R. J. Baxter, *Exactly Solved Models in Statistical Mechanics* (Academic Press, London, 1982).
12. F. G. Frobenius, *Gesammelte Abhandlungen*, Section 79 (Springer, Berlin, 1968).
13. C. Jayaprakash and A. Sinha, *Nucl. Phys. B* **210**:93 (1982).
14. C. N. Yang and C. P. Yang, *Phys. Rev.* **150**:321, 327 (1966).
15. E. R. Hansen, *A Table of Series and Products* (Prentice-Hall, Englewood Cliffs, New Jersey, 1975).
16. H. W. J. Blöte and H. Hilhorst, *J. Phys. A* **15**:L631 (1982).
17. I. S. Gradshteyn and I. M. Ryzhik, *Table of Integrals, Series and Products* (Academic Press, Orlando, Florida, 1980).
18. M. Abramowitz and I. A. Stegun, *Handbook of Mathematical Functions* (Dover, New York, 1965).